

# Two Methods for Reducing the Error-Floor of LDPC Codes

Stefan Ländner<sup>y</sup>, Thorsten Hehn<sup>z</sup>, Olgica Milenkovic<sup>y</sup>, and Johannes B. Huber<sup>z</sup>

<sup>y</sup>University of Colorado, Boulder, CO, USA

<sup>z</sup>University of Erlangen-Nuremberg, Erlangen, Germany

## Abstract

We investigate two techniques for reducing the error-floor of low-density parity-check codes under iterative decoding. Both techniques are developed based on comprehensive analytical and simulation studies of combinatorial properties of trapping sets in codes on graphs. The first technique represents an algorithmic modification of belief-propagation based on data fusion principles and specialized message averaging methods. The second technique relies on identifying redundant parity-check matrices of codes that do not contain small trapping sets. In the latter context we introduce the notion of the trapping redundancy of a code and show how decoding with redundant parity-check matrices can lead to reductions of error rates exceeding an order of magnitude. Our findings are described on the well known [2640;1320] Margulis code.

**Index Terms:** Averaged Decoding, Belief Propagation, Data Fusion, LDPC Codes, Margulis Codes, Trapping Redundancy, Trapping Sets.

## 1 Introduction

Low-density parity-check (LDPC) codes are a class of error-control codes known for their excellent performance when used for signalling over discrete, memoryless channels with moderate noise levels. In addition to their capacity-approaching performance, LDPC codes are also well suited for low-complexity iterative decoding, which makes them strong candidates for use in many modern communication and storage systems. Nevertheless, there exists one significant limiting factor for the successful employment of LDPC codes, which is the presence of *error floors* in their error-rate curves. The error floor represents a sudden change in the slope of the error curve that appears at moderate to high signal-to-noise ratios (SNRs). This change in slope makes the error rate of the codes decay very slowly, therefore reducing their effectiveness in systems which require extremely reliable communication. Many useful classes of LDPC codes, including those based on Cayley graphs [1], array codes [2], codes based on certain types of designs [3], and many random-like codes, have error-floors at relatively large bit error rates (BERs). For many other codes, error-floors lie in BER regions out of reach of standard simulation techniques, which makes them hard to detect but nevertheless very likely to occur.

---

Part of this work was presented at WirelessComm 2005, Maui, Hawaii, USA, and at the Globecom Conference 2006, San Francisco, California, USA. This work was supported in part by NSF Grant CCF-0514921 awarded to Olgica Milenkovic, by a research fellowship from the Institute for Information Transmission, University of Erlangen-Nuremberg, Erlangen, Germany, awarded to Stefan Ländner, and by a German Academic Exchange Service (DAAD) fellowship awarded to Thorsten Hehn.

The behavior of message-passing decoders in the error floor SNR region has been the subject of intense research activity. The error-floor was first investigated in terms of its relationship to near codewords, stopping sets, and trapping sets in [4, 5, 6]. Stopping and trapping sets were described in a general analytical setting in terms of *pseudocodewords* in *graph covers* of LDPC Tanner graphs [7]. Pseudocodewords are also known to influence the behavior of other classes of decoding algorithms for linear block-codes, such as linear programming decoding [8]. In both scenarios, pseudocodewords represent specialized variable node configurations which, when corrupted by certain low-probability noise samples, tend to cause failures of iterative decoders that do not occur during maximum likelihood (ML) decoding [9, 10]. Alternatively, pseudocodewords represent spurious configurations that exhibit similar properties as codewords, but on an “expanded” graphical representation of the code termed a *cover* [7]. This extended representation can be seen as arising due to the local nature of belief propagation (BP) decoding.

A computational technique for identifying pseudocodewords based on statistical physics techniques, termed the *instanton method*, was described in [11, 12], while another technique based on the well known *impulse method* was described in [13]. In both cases, pseudocodewords and their corresponding *worst case noise configurations* can be viewed as vectors pointing towards the shortest “exit point” from the decision region of a valid codeword.

Unfortunately, there exist no known techniques that allow for simple identification of all trapping sets and pseudocodewords in a code. As an example, the techniques described in [11, 13] are based on time-consuming computer-search strategies that are not guaranteed to succeed in identifying *all* pseudocodewords in long LDPC codes that can significantly contribute to the error-floor. It is therefore of interest to develop alternative techniques for analyzing trapping sets and error-floors and combat their detrimental effects on the performance of codes in a more efficient manner.

We propose to investigate two different approaches to eliminating trapping sets from a LDPC decoding graph. These approaches are based on purely *combinatorial* studies and they can be cast in a simple coding-theoretic framework, which distinguishes them from more evolved methods invoking results from statistical physics [12, 14, 15]. The first of the proposed approaches is algorithmic, and it aims to make the decoding process transparent to the existence of trapping sets/pseudocodewords. The second method is coding-theoretic, and it aims to identify the best decoding graph for a code with respect to the incidence rate of trapping sets. Within these two settings, we analyze *averaged decoding methods* as well as the *trapping redundancy of codes*. Our contributions regarding these problems are twofold:

We identify generalizations of iterative decoding algorithms that reduce the flow of erroneous information from and to the trapping set variables. These generalizations can be either viewed as belief propagation algorithms with

memory or belief propagation algorithms that employ data fusion principles [16]. At the same time, they can be seen as an application of mathematical methods aimed for handling divergent series [17]. Techniques of this form were first proposed by the authors in [18], and were analyzed independently and in a different context in [7, 15, 19].

We describe methods for selecting redundant rows for the parity-check matrix of a code that ensure error-free decoding of trapping set variables. In this setting, we introduce the notion of the *trapping redundancy of a code*, and provide analytical upper bounds on the values of these code parameters. The trapping redundancy represents an extension of the notion of the *stopping redundancy*, first described in [20]. We also identify classes of codes for which the trapping redundancy is small compared to the code length.

Although the work described in this paper represents a case-study of the Margulis [2640,1320] code, most of the described ideas and techniques can be adapted to apply to more general classes of codes as well.

The paper is organized as follows: Section 2 provides definitions and terminology related to LDPC codes and trapping sets that is used throughout the paper. It also gives a detailed description of the iterative decoding algorithm used for decoding and analyzing the trapping set phenomena. In Section 3, we describe the class of *averaged* BP algorithms, and show that their error thresholds do not exceed the thresholds of standard BP decoders. The influence of redundant parity-check equations on the structure of trapping sets and the performance of BP decoding is studied in Section 4. Analytical results pertaining to the central problems of the paper are described in the same section as well as in Section B. Proofs of a selected set of results are given in Appendix A and Appendix B.

## 2 Definitions, Background, and Terminology

We start by providing a comprehensive description of the message-passing algorithm used for studying the error-floor phenomena. Although message passing is by now a standard decoding technique [21], it is worth pointing out that the characteristics of decoding errors depend on the particular implementation of the algorithm and the accompanying message processing techniques<sup>1</sup> [23]. The discussion regarding message passing algorithms is followed by a brief introduction to trapping sets, their properties, and classification.

### 2.1 Belief-Propagation Algorithm

Decoding of LDPC codes is standardly performed in terms of an iterative algorithm that describes the protocol for exchanging reliability messages between the variable nodes and the check nodes of a bipartite Tanner graph [24]. Such

---

<sup>1</sup>Such as quantization [22].

an algorithm is known as a message passing (MP) algorithm, belief-propagation (BP) algorithm, or equivalently, the sum-product (SP) algorithm. The particular implementation of the product-sum algorithm used for our study is available at [25]. The software tool [25] utilizes the sum-product decoder described in [26].

Throughout the remainder of the paper we use  $H$  to denote the parity-check matrix of a binary  $[n; k; d]$  LDPC code  $C$ , and  $\mathcal{G}(H)$  to denote its corresponding bipartite Tanner graph. The columns of  $H$  are indexed by the elements of the set of variable (left-hand side) nodes  $\mathcal{N}$  of  $\mathcal{G}(H)$ , while the rows of  $H$  are indexed by the set of check (right-hand side) nodes  $\mathcal{M}$  of  $\mathcal{G}(H)$ . Furthermore, it is assumed that a codeword in  $C$ ,  $\mathbf{x} = (x_1; x_2; \dots; x_n)$ , is transmitted over an additive white Gaussian noise (AWGN) channel with noise variance  $\sigma^2$ . The signal-to-noise ratio (SNR) of the system is give by  $10\log_{10}(E_b/\sigma^2)$ , where  $E_b$  denotes the energy per coded bit.

Let us denote the set of variable nodes neighboring a check node indexed by  $c$  by  $\mathcal{N}(c) = \{i : H_{ci} = 1\}$ . Similarly, denote the set of check nodes neighboring a variable node indexed by  $v$  by  $\mathcal{M}(v) = \{j : H_{jv} = 1\}$ ; the notation  $\mathcal{M}(v)_{nc}$  is reserved for the set  $\mathcal{M}(v)$  excluding the check node  $c$ . During BP decoding, two types of probabilistic messages  $q_{cv;x_v}$  and  $r_{cv;x_v}$  are exchanged between a check node  $c$  and a variable node  $v$  if and only if the parity-check matrix has a nonzero entry at the respective position,  $H_{cv} = 1$ . The message  $q_{cv;x_v}$  represents the probability that variable  $v$  of the transmitted codeword is  $x_v$  ( $x_v \in \{0, 1\}$ ) given the information provided by all check nodes incident to variable node  $v$ , excluding  $c$  and the channel output corresponding to the variable  $x_v$ . The message  $r_{cv;x_v}$  represents the probability of check node  $c$  being satisfied, provided that the variable  $v$  has value  $x_v$  and all other variables incident to the check node have a separable distribution. The probabilities  $q_{cv;x_v}^{(\ell)}$ , where the superscript  $(\ell)$  indicates the iteration index, are initialized to the prior channel probabilities according to  $q_{cv;0}^{(0)} = p_{v;0} = P(x_v = 0)$ , and  $q_{cv;1}^{(0)} = p_{v;1} = P(x_v = 1) = 1 - p_{v;0}$ .

The *horizontal step* of the  $\ell$ -th iteration of the algorithm is initiated by computing the probabilities  $r_{cv;x_v}^{(\ell)}$ . This is accomplished in terms of the *fast implementation* approach described in [26]: first, the difference of the probabilities,  $\delta r_{cv} = r_{cv;0}^{(\ell)} - r_{cv;1}^{(\ell)}$ , is found according to

$$\delta r_{cv} = \prod_{v' \in \mathcal{N}(c)} (q_{cv';0}^{(\ell-1)} - q_{cv';1}^{(\ell-1)}) = (q_{cv;0}^{(\ell-1)} - q_{cv;1}^{(\ell-1)}); \quad (1)$$

Whenever a denominator equal to zero is encountered, its value is reset to  $10^{-20}$  in order to avoid division by zero. The horizontal step is terminated by computing  $r_{cv;0} = \frac{1}{2}(1 + \delta r_{cv})$  and  $r_{cv;1} = \frac{1}{2}(1 - \delta r_{cv})$ . Since in the iterations to follow, the values of  $r_{cv;0}$  and  $r_{cv;1}$  will appear in the denominator of certain quotients, at each step they are lower-bounded by  $10^{-20}$ , but so as to obey the constraint  $r_{cv;0} + r_{cv;1} = 1$ .

During the *vertical step* of the  $\ell$ -th iteration of the BP algorithm, the values of  $q_{cv;0}$  and  $q_{cv;1}$  are updated as follows.

First, the *pseudoposterior probabilities* of  $x_v$  being zero or one are found according to

$$\begin{aligned} q_{v;0}^{(\ell)} &= \alpha_v p_{v;0} \prod_{c \in \mathcal{M}(v)} r_{cv;0}^{(\ell)} \\ q_{v;1}^{(\ell)} &= \alpha_v p_{v;1} \prod_{c \in \mathcal{M}(v)} r_{cv;1}^{(\ell)}; \end{aligned} \quad (2)$$

where  $\alpha_v$  is chosen so as to ensure  $q_{v;0}^{(\ell)} + q_{v;1}^{(\ell)} = 1$ . The probabilities described above are used for tentative decoding. The algorithm stops if the hard-decision values of the pseudoposterior probabilities represent a valid codeword. Otherwise, from the pseudoposterior probabilities, the values of  $q_{cv;0}$  and  $q_{cv;1}$  are calculated according to the equations:

$$\begin{aligned} q_{cv;0}^{(\ell)} &= \alpha_{cv} p_{v;0} q_{v;0}^{(\ell)} / r_{cv;0}^{(\ell)} \\ q_{cv;1}^{(\ell)} &= \alpha_{cv} p_{v;1} q_{v;1}^{(\ell)} / r_{cv;1}^{(\ell)}; \end{aligned} \quad (3)$$

where  $\alpha_{cv}$  is chosen so that  $q_{cv;0}^{(\ell)} + q_{cv;1}^{(\ell)} = 1$ . These probabilities are passed on to the horizontal step of the next iteration.

Note that minor differences in the implementation of this algorithm can result in substantially different behavior of the decoder at moderate and high SNR values, where one expects to encounter probability values very close to zero and one. Especially important is the effect of thresholding (quantizing) the probability values close to zero [5]. We restrict our attention to the BP algorithm described above, and its log-likelihood ratio version (LLR). The only difference between the two algorithms is that the latter uses messages of the form  $\lambda_v^{(\ell)} = \log \frac{p_0^{(\ell)}}{p_1^{(\ell)}}$ , where  $p_i^{(\ell)}; i = 0;1$  equals either  $q_{i;x_v}^{(\ell)}; i = 0;1$ , or  $p_{i;x_v}^{(\ell)}; i = 0;1$ , rather than the probabilities themselves.

## 2.2 Near-Codewords and Trapping Sets

The error-floor phenomenon was first described by MacKay and Postol in [4], where it was observed that the bit error rate (BER) curve of the  $[2640;1320]$  Margulis code exhibits a sudden change of slope at SNRs approximately equal to 2.4 dB. This change of slope was attributed to the existence of *near-codewords* in the Tanner graphs of the Margulis code with a parity-check matrix  $H$  described in [1]. Near codewords are vectors  $\mathbf{y}$  of small weight with syndromes  $\mathbf{s}(\mathbf{y}) = H\mathbf{y}$  that also have small weight. In his seminal paper [5], Richardson analyzed the effect of near-codewords on the behavior of various classes of decoders and for a group of channels, and introduced the notion of *trapping sets* to describe configurations in Tanner graphs of codes that cause failures of specific decoding schemes. There exist many different groups of trapping sets. For example, trapping sets of maximum likelihood (ML) decoders are the *codewords* of the code; trapping sets of iterative decoders used for messages transmitted over the binary erasure channel are stopping sets [6]. For the AWGN channel and BP decoding, no simple characterization of trapping sets is known. Nevertheless,

extensive computer simulations reveal that a large number of trapping sets for this channel/decoder combination can be described in a simple and precise setting. Henceforth, we use the notion trapping set to refer exclusively to a set of the form described below.

**Definition 2.1.** A  $(a;b)$  trapping set  $\mathcal{T}$  is a configuration of  $a$  variable nodes, for which the subgraph in  $\mathcal{G}(H)$  induced by  $\mathcal{T}$  and its neighbors contains  $b \geq 0$  odd-degree check nodes<sup>2</sup>. An *elementary*  $(a;b)$  trapping set is a trapping set for which all check nodes in the subgraph induced by  $\mathcal{T}$  and its neighbor have either degree one or two, and there are exactly  $b$  degree-one check nodes.

It is straightforward to see that the number of trapping sets in a Tanner graph depends on the particular choice of the parity-check matrix of the code used to define this graph. We therefore define trapping sets for a specific choice of the parity-check matrix as follows.

**Definition 2.2.** For a given  $m \times n$  matrix  $H = (h_{i,j})$  with  $1 \leq i \leq m, 1 \leq j \leq n$ , the projection of a set of  $h$  columns indexed by  $j_1, j_2, \dots, j_h$  is defined as an  $m \times h$  subarray of  $H$  consisting of the elements  $h_{i,j}; 1 \leq i \leq m; j = j_1, j_2, \dots, j_h$ . A  $(a;b)$  trapping set  $\mathcal{T}$  of  $H$  is a set of  $a$  columns of  $H$  with a projection that contains  $b$  odd-weight rows. An *elementary*  $(a;b)$  trapping set is a trapping set for which all non-zero rows in the projection have either weight one or two, and exactly  $b$  rows have weight one.

Based on extensive computer simulations performed in [5] and in [18], it was observed that the majority of trapping sets that exhibit a strong influence on the error-floor level are of elementary form. Furthermore, although check nodes of odd degree larger than one are possible, they seem to be very unlikely within small trapping sets [27]. We henceforth focus our attention only on elementary trapping sets. An example of the incidence structure corresponding to an elementary  $(5;1)$  trapping set of a  $(3; \infty)$  regular LDPC code is shown below. The variables  $v_i$  and  $c_i$  represent the indices of the variable and check nodes in the trapping set. The number of even-degree check nodes in the trapping set is equal to seven. This follows from the simple observation that in regular LDPC codes with variable degrees  $d_v$ , any elementary  $(a;b)$  trapping set has to include  $(d_v - a - b)/2$  “satisfied” checks.

---

<sup>2</sup>The case  $b = 0$  corresponds to *codewords*. Consequently, we deal with the  $b > 0$  case only.

	$v_1$	$v_2$	$v_3$	$v_4$	$v_5$
$c_1$	1	0	0	0	0
$c_2$	1	1	0	0	0
$c_3$	1	0	1	0	0
$c_4$	0	1	0	1	0
$c_5$	0	1	0	0	1
$c_6$	0	0	1	1	0
$c_7$	0	0	1	0	1
$c_8$	0	0	0	1	1

(4)

### 2.3 Trapping Sets And The Error-Floor Phenomena

The influence of trapping sets on the onset of error-floors in LDPC codes can be attributed to the following phenomena, related both to the properties of the code graph and decoding algorithm, as well as to realization of certain special channel-noise configurations. In the initial stage of BP decoding, due to the presence of special low-probability noise samples [11], variable nodes internal to one particular trapping set (termed the *initial trapping set*) experience a large increase in reliability estimates for incorrect bit values. This information gets propagated to other variable nodes in the trapping set, some of which already have unreliable bit estimates themselves. After this initial biasing, external variables usually start to correct their initially incorrect estimates. By that time, the variable nodes in a trapping set have already significantly biased their decisions towards the wrong values. Since there are very few check nodes capable of detecting errors within trapping sets, this erroneous information persists in the graph until the end of the decoding process. Furthermore, the unreliable estimates in trapping sets sometimes get “amplified” and/or “exported” to the variable nodes external to the trapping set. The degree of influence of the trapping set on the external variables (and vice versa) is an important factor that influences the behavior of trapping sets under iterative decoding, and it cannot be described in a simple manner. This is why the complete failure characterization of iterative decoders is not possible in terms of using trapping sets only. Nevertheless, it can be shown that for the  $[2640;1320]$  Margulis code, most decoding errors are confined to subsets of either 12 or 14 variables for which the subgraph induced by these variable nodes and their neighbors contains exactly four unsatisfied checks [5]. This finding can be explained in part by the fact that the presence of *only four* check nodes capable of detecting errors does not suffice to ensure correct decoding of the corresponding trapping variables.

Based on the estimates given in [5], 75% of all frame errors occurring at SNRs close to 2.4 dB can be attributed to subsets with 12 variables, while approximately 23% of the frame errors arise due to subsets with 14 variables. All subsets with 14 variables were found to represent two-variable extensions of trapping sets with 12 variables. The elementary trapping sets in the Margulis code can, in general, be classified into three groups: *point*, *periodic*, and *aperiodic* elemen-

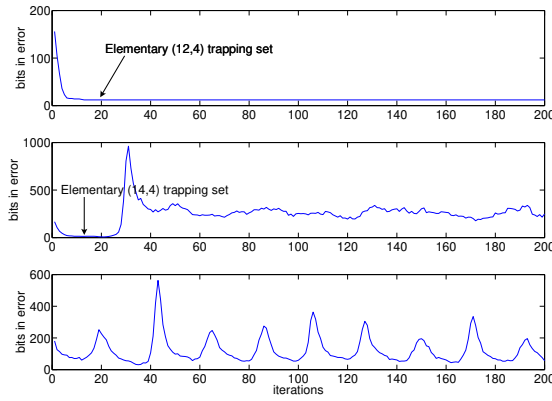


Figure 1: Frames with trapping set errors, under sum-product decoding.

tary trapping sets. *Point* trapping sets represent subsets of variable nodes that contain all erroneous variables encountered starting from some iteration  $l_{\text{start}}$  up to the maximum number of iterations of the decoder,  $l_{\text{max}}$ . The (12;4) and (14;4) sets identified in [4, 5] and described above are of this form. *Periodic* trapping sets are varying subsets of the variable nodes that switch from erroneous to error-free values in a near-periodic fashion. Such sets occur very rarely, and are usually not detected during VLSI decoder prototyping [23]. Finally, *aperiodic* trapping sets represent subsets of variable nodes that are in error at only one stage of the decoding process, and are never revisited again. Figure 1 gives an illustration of these three different forms of trapping sets. The graphs show the number of variables in error per iteration of BP decoding, for three codewords of the Margulis code with errors confined to a point trapping set, an aperiodic trapping set, and a periodic trapping set.

## 2.4 Algorithmic Techniques

So far, several simple algorithmic techniques for eliminating the negative influence of pseudocodewords/trapping sets on the performance of iterative decoders were proposed. The first results in this direction were described in [28, 29], where it was shown that message damping can reduce the performance gap between the sum-product and the min-sum as well as some modified BP algorithms. Iterative decoders with damping features were also considered for decoding Reed-Solomon codes [30, 31, 32] and linear block codes in general [33]. The idea of using message damping to reduce the error floor can be traced back to the work by Laendner and Milenkovic [18] and Pretti [15]. In these papers, it was shown that *message averaging* or *message damping* can significantly lower the error-floor in terms of slowing down the propagation of erroneous information to and from trapping set variables. More recently, Vontobel and Koetter [7] proposed a similar modification for iterative decoding which consists in using weighted averages of the log-likelihood



ratio messages over two consecutive iterations. The same approach was put in a statistical physics framework in the more recent work described in [11, 12].

Here, we extend and generalize our findings from [18] and show that damping and averaging can be viewed as special instances of data fusion performed on messages passed through Tanner graphs. Furthermore, we study the impact of various forms of data fusion techniques on the error-floor characteristics of the Margulis codes. A detailed description of averaging, damping and data fusion is provided in the next section. It is worth pointing out that our techniques differ from the related methods outlined above in so far that they are completely combinatorial in nature and do not require complicated adaptation strategies.

## 2.5 Redundant Parity-Check Matrices

The Tanner graph of a linear  $[n; k; d]$  code  $C$  can be described in terms of parity-check matrices of different forms. A parity-check matrix is usually chosen so that its rows represent basis vectors of the subspace corresponding to  $C^\perp$ . For the purpose of iterative decoding, such parity-check matrices may not represent a good choice. This is due to the fact that such matrices are either irregular or that they contain a large number of stopping sets [20, 34]. Consequently, many parity-check matrices used for iterative decoding are *redundant* - i.e., they contain more than  $n - k$  rows (of course, the rank of a redundant parity-check matrix still has to equal to  $n - k$ ). Examples include the matrices described in [20, 35, 36] that do not contain stopping sets of size smaller than  $d - 1$ .

Henceforth, we use the phrases *redundant parity-check matrix* to describe a parity-check matrix with  $> n - k$  rows. In a redundant parity-check matrix, there may exist one or more rows that represent linear combinations of other rows. On the other hand, a full-rank parity-check matrix of minimum dimensions  $(n - k) \times n$  will be simply referred to as a *parity-check matrix*. Rows added to a parity-check matrix will be called *redundant rows*. Redundant parity-check matrices can be used to impose more restrictive constraints on the structure of their corresponding Tanner graphs. As will be shown in Section 4, judiciously chosen redundant parity-check matrices can be used to lower the error floor of the Margulis code. This is achieved in terms of rendering the structure of small trapping sets so as to make the number of their unsatisfied checks sufficiently large. In this context, our results can be seen as a generalization of the findings in [20] for the case of trapping sets. An analytical study of the influence of redundant rows on the parameters of small trapping sets is described in Section 4.4.

### 3 Message Averaging and Damping

#### 3.1 Motivation

There are many intuitive reasons why averaging messages passed during different iterations of belief propagation can lead to improved BER performance in the error floor regime. One explanation follows from viewing averaging as *message damping*, which is a well known technique from statistical physics and dynamical systems theory used for controlling chaotic behavior of a system. Averaging can also be viewed as a method for adding memory to the decoding process and combining *expert opinion* [16] from the past and present in order to increase the reliability of the decision. Yet another explanation follows from the theory of divergent series [17], where various forms of averaging are used to convert oscillating sums into convergent series.

Let us start by describing the notion of message damping in a statistical physics framework [15]. It is well known that BP decoding is a special instance of the *Bethe-Kikuchi* method for estimating the Boltzmann distribution of an appropriately defined thermodynamical system [37]. The stability of the Bethe-Kikuchi method can be improved in terms of *probability damping*. Damping can be performed in several different ways, including arithmetic averaging, geometric averaging, and normalization. In the context of estimating the Boltzmann distribution, the updates of probabilities of variable nodes are computed within the following setup. First, variable nodes are viewed as random variables  $X_i; i = 1; \dots; n$ ; with an interaction pattern described in terms of the Hamiltonian operator

$$\mathbf{H} = \sum_{\mathcal{N}(c)} h(X_{\mathcal{N}(c)}):$$

Here, the sum ranges over all sets  $\mathcal{N}(c)$  that represent collections of variable nodes connected to a check node  $c$ , and  $h()$  denotes the check function Hamiltonian [15] that may also account for external fields operating on the nodes (i.e. for noise added to the variable nodes). Consequently, each set  $\mathcal{N}(c)$  corresponds to one parity-check equation, and  $X_{\mathcal{N}(c)}$  denotes the collection of random variables checked by  $c$ . The Bethe free energy of the system described above can be written as

$$F[\mathbf{p}] = \sum_{\mathcal{N}(c)} \sum_{X_{\mathcal{N}(c)}} p_{\mathcal{N}(c)}(X_{\mathcal{N}(c)}) [h_{\mathcal{N}(c)}(X_{\mathcal{N}(c)}) + \ln p_{\mathcal{N}(c)}(X_{\mathcal{N}(c)})] + \sum_i c_i \sum_{X_i} p_i(X_i) [h_i(X_i) + \ln p_i(X_i)]; \quad (5)$$

where  $p_i(X_i)$  denotes the marginal probability distribution of the variable  $X_i$ , and  $p_{\mathcal{N}(c)}(X_{\mathcal{N}(c)})$  denotes the marginal probability distribution of the collection of random variables  $X_{\mathcal{N}(c)}$ . The notation  $\mathbf{p}$  is reserved for the collection of all marginal distributions of the random variables  $X_i; i = 1; \dots; n$ . In addition,  $c_i = 1 - d_i$ , where  $d_i$  is the out-degree of the variable node associated with the variable  $X_i$ . The marginals of the Boltzmann distribution can be found in terms of an

iterative procedure which is equivalent to belief propagation decoding. Furthermore, the computation of the marginals can be modified so as to include damping of the following form [15]:

$$p_i^{j+1}(X_i) = p_i^j(X_i)^\gamma e^{-c_i h_i(X_i)} \prod_{a \in \mathcal{N}(c_i)} m_{a \rightarrow i}(X_i)^{\frac{\gamma}{1-\gamma}} :$$

The index  $j$  refers to the iteration number, while  $\mathcal{N}(c_i)$  is used to denote the set of check nodes neighboring the variable node corresponding to  $X_i$ .

It can be easily seen that damping represents a special form of *aggregation of probability distributions* [16]. Usually, probabilities from multiple observation systems (e.g. experts) are combined by using axiomatic approaches. One such approach was described in [38], and it can be dated back to Laplace. If  $P_i(\theta)$  denotes the probability distribution of a variable  $\theta$  as observed by the  $i$ -th expert system, then the combined probability distribution of the variable  $\theta$  can be computed as

$$P(\theta) = c \sum_{i=1}^n \omega_i P_i^r(\theta) ; \quad (6)$$

where  $c$  is a properly chosen normalization constant and  $r$  is a scaling factor which takes non-negative real values. If  $c = 1$  and  $r = 1$ , then the expert Equation (6) reduces to the so called *linear opinion pool* equation,

$$P(\theta) = \sum_{i=1}^n \omega_i P_i(\theta) : \quad (7)$$

Similarly, if  $r \rightarrow 0$ , then the expert equation results in a *logarithmic opinion pool*, for which

$$P(\theta) = c \prod_{i=1}^n P_i^{\omega_i}(\theta) : \quad (8)$$

The linear opinion pool satisfies the unanimity and marginalization property, while the logarithmic opinion pool satisfies the principle of *external Bayesianity* [16]. Linear pooling corresponds to arithmetic averaging, while logarithmic pooling corresponds to geometric averaging<sup>3</sup>. It is straightforward to see that the damping Equation 6 is a logarithmic opinion pool based on two experts, with weighting factors  $\omega_1 = \gamma$  and  $\omega_2 = 1 - \omega_1 = 1 - \gamma$ . Therefore, damping and other forms of averaging applied to messages of the belief propagation algorithm can be viewed as aggregation of message probabilities from several iterations, where “experts” correspond to “iterations”. Averaged decoding can also be viewed as belief propagation decoding with memory.

Due to its connection to general means, averaging can also be seen as a method for “summing” oscillating series [17]. A convergent series  $\sum_{i=1}^{\infty} a_i$  has the property that its partial sums,  $s_n = \sum_{i=1}^n a_i$ , represent a convergent series. In other

<sup>3</sup>The most general averaging technique consistent with the axioms of probability theory can be found in [39], although it will not be considered in this paper.

words,  $\lim_{n \rightarrow \infty} s_n = s < \infty$ . A series that is not convergent is called a *divergent* series [17]. Divergent series either have  $s = \infty$ , or they exhibit oscillating behavior, so that the defining limit does not exist (some authors, like Hardy [17], use the word “divergent” to refer to oscillating series only). An example of the latter form is the series  $+1; -1; +1; -1; \dots$ . Henceforth, we say that a series or sequence diverges if its limit exists, but is not finite. Similarly, we say that a series or sequence oscillates if the corresponding limit does not exist. Oscillating series may be converted into convergent or divergent series if *averaged with respect to several indices*. More precisely, oscillating series do not have a limit for their partial sums *only* under the constraint that the meaning of *sum* is taken in the standard manner. There are different summation methods that differ from standard summation. The best known of these techniques is the *Cesáro* method. A series  $\sum_{i=1}^{\infty} a_i$  is said to be Cesáro summable if and only if

$$s = \lim_{n \rightarrow \infty} \frac{s_0 + s_1 + \dots + s_n}{n+1} < \infty; \quad (9)$$

Clearly, Cesáro sums are nothing more than arithmetic averages of an increasing number of terms of the original series. More general weighted averaging techniques include the Borel method and the *Nörlund* methods [17]. In the latter case, one first defines a decreasing series of coefficients

$$\beta_n \geq 0; \beta_0 > 0; B_n = \beta_0 + \dots + \beta_n; \quad (10)$$

and then an average of the form

$$\frac{\beta_n s_0 + \beta_{n-1} s_1 + \dots + \beta_0 s_n}{\beta_0 + \beta_1 + \dots + \beta_n}; \quad (11)$$

where  $s_j = \sum_{i=0}^j a_i$ . Of special importance are *regular summability methods* [17]. A summability method is said to be *regular* if every series convergent or divergent in the standard setting is also convergent or divergent under the given summability method, and has the same limit in both cases. A regular method preserves the convergence properties of an infinite series. Clearly, Cesáro sums are regular, since  $\sum_{i=0}^{\infty} a_i = s$  implies that the limit in (9) also equals  $s$ . On the other hand, a Nörlund method is regular if and only if  $\beta_n/B_n \rightarrow 0$  as  $n \rightarrow \infty$ .

It is straightforward to see that all the above described mathematical techniques are based on the same underlying principles of “smoothing out” oscillating behavior arising in dynamical systems, expert systems, and infinite series. In the context of belief propagation decoding, “smoothing” has a similar meaning. There, one sometimes encounters oscillating behavior of the probabilities prior to the trapping event, either due to numerical instabilities or to some of the inherent properties of the decoding algorithm. Therefore, averaging may be viewed as a means of controlling the oscillations in such a system. It can also be seen as a method for controlling the speed with which extrinsic information is passed from

one variable node to another. Finally, it represents a way to combine “expert opinions” from various subgraphs of the Tanner graph<sup>4</sup>.

In what follows, we refer to any form of a BP algorithm that uses some form of message averaging as an *averaged decoder*. In particular, we focus our attention on arithmetic and geometric averaging methods applied both to probabilities as well as to log-likelihood ratios passed by variable or check nodes. In order to keep the exposition focused, we present simulation results only for those techniques that were found to offer some advantage (computational or performance based) over other methods.

### 3.2 Averaged BP Decoding

Let us denote the *averaged probabilities* of a variable node  $v$  having value 0 and 1 at iteration number  $l$  by  $\hat{q}_{v;0}^{(l)}$  and  $\hat{q}_{v;1}^{(l)}$ , respectively. These probabilities are obtained by taking the average of  $l_{\text{av}}$  probability values assigned to node  $v$ , starting from the  $l_{\text{min}}$ -th iteration. More precisely, the average is taken over the pseudoposterior probability of the last iteration,  $q_{v;0}^{(l)}$  and  $q_{v;1}^{(l)}$ , and the averaged pseudoposterior probabilities of the  $l_{\text{av}} - 1$  previous iterations,  $\hat{q}_{v;0}^{(i)}$  and  $\hat{q}_{v;1}^{(i)}$ ,  $i = l - 1; l - 2; \dots; l - l_{\text{av}} + 1$ .

Define the averaged probability update rules as follows. For the first  $l_{\text{min}}$  iterations, no averaging is performed so that the averaged probabilities are equal to the probabilities given by (2), i.e.

$$\hat{q}_{v;0}^{(l)} = q_{v;0}^{(l)} \quad \hat{q}_{v;1}^{(l)} = q_{v;1}^{(l)} : \quad \text{for } l \leq l_{\text{min}} : \quad (12)$$

For iteration indices  $l_{\text{min}} < l < l_{\text{min}} + l_{\text{av}}$ , the message probability update rules are given by

$$\begin{aligned} \hat{q}_{v;0}^{(l)} &= g(q_{v;0}^{(l)}; \hat{q}_{v;0}^{(l-1)}; \hat{q}_{v;0}^{(l-2)}; \dots; \hat{q}_{v;0}^{(l_{\text{min}})}) \\ \hat{q}_{v;1}^{(l)} &= g(q_{v;1}^{(l)}; \hat{q}_{v;1}^{(l-1)}; \hat{q}_{v;1}^{(l-2)}; \dots; \hat{q}_{v;1}^{(l_{\text{min}})}) ; \end{aligned} \quad (13)$$

where  $q_{v;0}^{(l)}$  and  $q_{v;1}^{(l)}$  are used to denote the message probabilities passed at the  $l$ -th iteration, computed from the averaged probabilities  $\hat{q}_{v;0}^{(i)}$  and  $\hat{q}_{v;1}^{(i)}$ ,  $l_{\text{min}} < i < l_{\text{min}} + l_{\text{av}}$ , and the update rules (12) and (13). The function  $g(\cdot)$  may take different forms for different averaging strategies, and it may be applied to the probabilities  $r_{cv;v}$ , rather than the probabilities  $q_{v;0}^{(l)}$ . Some specific choices for  $g(\cdot)$  will be described at the end of this section.

---

<sup>4</sup>It is to be observed that for each iteration, the decoder operates on a different form of an *unwrapped coding tree/graph*. Consequently, averaging over several iterations corresponds to averaging message values obtained from several different graphical structures.

For all other iteration indices  $l = l_{\min} + l_{\text{av}}$ , the averaged probability update equations are of the form

$$\begin{aligned}\hat{q}_{v;0}^{(l)} &= g(q_{v;0}^{(l)}; \hat{q}_{v;0}^{(l-1)}; \dots; \hat{q}_{v;0}^{(l_{\text{av}}+1)}) \\ \hat{q}_{v;1}^{(l)} &= g(q_{v;1}^{(l)}; \hat{q}_{v;1}^{(l-1)}; \dots; \hat{q}_{v;1}^{(l_{\text{av}}+1)}) : \end{aligned} \quad (14)$$

During one iteration of averaged message passing, the averaged probabilities  $\hat{q}_{v;0}^{(l)}$  and  $\hat{q}_{v;1}^{(l)}$  are sent to the parity-check nodes and updated in a standard manner<sup>5</sup>:

$$\begin{aligned}q_{cv;0}^{(l)} &= \alpha_{cv} \hat{q}_{v;0}^{(l)} = r_{cv;0} \\ q_{cv;1}^{(l)} &= \alpha_{cv} \hat{q}_{v;1}^{(l)} = r_{cv;1} ; \end{aligned} \quad (15)$$

where  $\alpha_{cv}$  is chosen such that  $\hat{q}_{cv;0}^{(l)} + \hat{q}_{cv;1}^{(l)} = 1$ . Note that in the equations above we made a slight abuse of notation by denoting the *most recent* - i.e. *current* probability messages, calculated using the averaged probabilities of the previous iterations, by  $q_{cv;0=1}^{(l)}$ ,  $r_{cv;x_n}$ , and  $q_{v;x_v}^{(l)}$ . The probabilities  $q_{v;0}^{(l)}$  and  $q_{v;1}^{(l)}$  represent messages obtained before applying the averaging update function  $g$ , and they are evaluated according to Equation (2).

We focus our attention on three different forms of the averaging function  $g()$ , and use  $p$  to denote either the  $q$  or  $r$  probabilities defined in the previous sections. Which of these two probabilities one is averaging over will be apparent from the context in which the formulas are used.

a. Arithmetic averaging of probabilities:

$$g_1(p_1; p_2; \dots; p_L) = \frac{1}{L} (p_1 + p_2 + \dots + p_L) \quad (16)$$

b. Geometric averaging of probabilities:

$$g_2(p_1; p_2; \dots; p_L) = \sqrt[p]{p_1 p_2 \dots p_L} \quad (17)$$

c. Weighted arithmetic averaging of probabilities:

$$g_3(p_1; p_2; \dots; p_L) = \frac{1}{\sum_{i=1}^L \beta_i} (\beta_L p + \beta_{L-1} p + \dots + \beta_1 p) ; \quad (18)$$

where the weighting coefficients  $\beta_i$ ,  $1 \leq i \leq L$  are chosen as described in definition of a Nörlund sum.

Note that averaging can result in a slower speed of message changes. To minimize this undesirable effect of averaging one can make the averaging algorithm follow some adaptive set of rules. In this context, *adaptive* refers to the ability of the algorithm to initiate the averaging process at each variable node *individually*, and only in the case that the absolute change in pseudoposterior probabilities during two adjacent iterations exceeds a given threshold  $\theta$ .

<sup>5</sup>Note that if averaging is performed on the probabilities  $r_{cv;x_v}$ , then this step has to be replaced by one in which these probabilities are computed according to the rules prescribed by the function  $g()$ .

### 3.3 Thresholds of Averaged BP Algorithms

#### Background

The error-correcting performance of BP decoders is most easily analyzed in terms of density evolution (DE) [40]. DE can be used to find capacity-approaching degree distributions for irregular LDPC codes as well as to determine the decoding threshold for a wide variety of discrete, memoryless channels. While DE is straightforward to perform for the case of the BEC channel, it can be a complex undertaking for other channels such as the additive white Gaussian noise (AWGN) channel, unless certain analytical approximations are made. Chung, Richardson, and Urbanke [41] showed that one such approximation for DE of the message passing algorithm for an AWGN channel consists in modelling the messages as Gaussian random variables in a one-dimensional parameter space. For completeness, we briefly summarize the basic equations behind the Gaussian approximation for DE, and then proceed to use these results in order to study the threshold of averaged decoders (to be rigorously defined below). We use Gaussian approximation techniques to show that various forms of averaging do not increase the decoding threshold of LDPC codes and consequently do not exhibit a negative influence on the codes performance in the waterfall region. On the other hand, as will be shown in Section 3.4, averaging may result in a significant decrease in the error floor of codes.

Let us recall the LLR version of the message passing algorithm described in Section 2.1, and for the moment, assume that averaging is performed at the variable nodes. In this case, the messages of interest are of the form  $\mathbf{v}^{(\ell)} = \log \hat{q}_{v;0}^{(\ell)} = \hat{q}_{v;1}^{(\ell)}$ . At each variable node, its corresponding channel message  $\mathbf{v}_{v;0}^{(\ell)}$  and all the messages  $\mathbf{v}_{v;c_i}^{(\ell)}; i = 1; 2; \dots; d_v$  from its neighboring check nodes  $c_i \in \mathcal{M}(v)$  are summed up to obtain

$$\mathbf{v}^{(\ell+1)} = \mathbf{v}_{v;0}^{(\ell)} + \sum_{i=1}^{d_v-1} \mathbf{v}_{v;c_i}^{(\ell)} \quad (19)$$

By using the duality property of variable and check nodes, one similarly obtains

$$\tanh \frac{\mathbf{c}^{(\ell+1)}}{2} = \prod_{j=1}^{d_c-1} \tanh \frac{\mathbf{v}_j^{(\ell)}}{2}; \quad (20)$$

where  $\mathbf{v}_j^{(\ell)}$  denote messages from variable nodes  $v_j \in \mathcal{N}(c)$ .

The LLRs of messages at the output of the AWGN channel have a Gaussian distribution, with mean and variance  $2\sigma^2$  and  $4\sigma^2$ , respectively. Although the messages  $\mathbf{v}_{v;c_i}^{(\ell)}$  are, in general, neither Gaussian nor independent, the random variables  $\mathbf{v}^{(\ell+1)}; l = 1; 2; \dots$  can be approximated by Gaussian random variables. A similar model is used for the random variables  $\mathbf{c}^{(\ell+1)}$ , although these variables are provably non-Gaussian [41]. To simplify analysis, let us assume that the messages  $\mathbf{v}^{(\ell)}$  and  $\mathbf{c}^{(\ell)}$  are Gaussian random variables [42, 43], with means  $m_v^{(\ell)}$  and  $m_c^{(\ell)}$ , and variance equal to twice the

mean. The variable node update equation can then be rewritten as

$$m_v^{(q)} = m_{v_0} + (d_v - 1)m_c^{(q-1)};$$

To obtain the update equation for  $m_c^{(q)}$ , one first has to find the expected values of both sides of Equation (20). Then, the expected value of the right hand side of (20) is expressed in terms of a continuous, monotonically decreasing function  $\phi(x)$  on  $[0; \infty)$  with limits  $\phi(0) = 1$  and  $\phi(\infty) = 0$ , so that

$$m_c^{(q)} = \phi^{-1} \left( 1 - \frac{1}{d_c - 1} \phi(m_{v_0} + (d_v - 1)m_c^{(q-1)}) \right); \quad (21)$$

where two particular approximations for  $\phi$  can be found in [41]. The expression above can be recast as

$$m_c^{(q)} = f(m_{v_0}; m_c^{(q-1)}); \quad (22)$$

Consequently, the check node update equation reduces to  $t_l(s) = f(s; t_{q-1}(s))$ , with  $t_l(s) = m_c^{(q)}$ . The same arguments can be used to derive the update rules for variable and check nodes in irregular codes, by replacing Gaussian variables by appropriate Gaussian mixtures [41].

**Theorem 3.1.** [41] *For a fixed  $s$ ,  $t_l(s)$  diverges if and only if*

$$t_l(s) < f(s; t_l(s)); \text{ i.e., } t_l(s) > t_{q-1}(s) \geq l - l_0; \text{ for some } l_0 > 0;$$

Define the threshold  $s^2$  as the infimum of all  $s$  in  $\mathbb{R}^+$  such that  $t_l(s)$  diverges, i.e. such that  $\lim_{l \rightarrow \infty} t_l(s) = \infty$ . Then

$$s^2 = \inf_{s \in \mathbb{R}^+} \lim_{l \rightarrow \infty} f(s; t_l(s)) = \infty; \quad (23)$$

The threshold is proportional to the inverse of the highest noise variance the decoder can tolerate. Since the function  $f(s; t)$  is monotonically increasing on both  $0 < s < \infty$  and  $0 < t < \infty$ , for all  $s > s^2$  and  $t_l(s) > t_l(s^2)$ ,  $t_l(s)$  diverges as well.

### Thresholds of Averaging Decoders

We show next that the sequence  $\hat{t}_l(s)$ , obtained from an update function that corresponds to certain forms of averaged decoding also diverges for all  $s > s^2$ , where  $s$  denotes the threshold of standard BP decoding. The word ‘‘averaged’’ refers to arithmetic averaging of probabilities (Equation (16)), geometric averaging of probabilities (Equation (17)), as well as Nörlund averaging (Equation (18)) with appropriate parameters  $l_{av}$  and  $l_{min}$ . We also show that the decoding threshold does not increase if arithmetic/geometric averaging of log-likelihood ratios is performed. Under suitable conditions, the findings hold for averaging either over variable or check messages. We provide proofs for a selected set of methods



applied to check nodes. We omit the proofs for averaging techniques operating on variable nodes, since these are either fairly straightforward to derive or since they follow from the corresponding results derived for check node averages.

**Case 1:** Consider a sequence  $\hat{t}_l(s)_{l=0}^{\infty}$  and initialize it as follows:  $\hat{t}_0(s) = t_0(s) = 0$ ,  $\hat{t}_1(s) = t_1(s) = f(s; t_0(s))$ . Then, for all  $l \geq 2$ , let

$$\hat{t}_l(s) = \frac{1}{l} (f(s; \hat{t}_{l-1}(s)) + \hat{t}_{l-1}(s) + \hat{t}_{l-2}(s) + \dots + \hat{t}_1(s)); \quad \text{for } l \leq l_{av}; \quad (24)$$

$$\hat{t}_l(s) = \frac{1}{l_{av}} (f(s; \hat{t}_{l-1}(s)) + \hat{t}_{l-1}(s) + \hat{t}_{l-2}(s) + \dots + \hat{t}_{l_{av}+1}(s)); \quad \text{for } l > l_{av}; \quad (25)$$

where  $f(s; t)$  is as defined above and  $l_{av} \geq 2$ .

**Lemma 3.1.** *The sequence  $\hat{t}_l(s)$  diverges for all  $s > s^2$ , i.e. a decoder with update Equations (24) and (25) has a noise threshold that is upper bounded by the threshold of the standard sum-product algorithm.*

The proof is given in Appendix A.1.

**Case 2:** We show next that geometric averaging of LLRs over  $l_{av}$  iterations does not increase the threshold of BP decoding. In this case, define a sequence  $\check{t}_l(s)_{l=0}^{\infty}$ , and initialize it according to  $\check{t}_0(s) = 0$  and  $\check{t}_1(s) = t_1(s) = f(s; t_0(s)) > 0$ . Let  $t_l(s)$  and  $f(s; t_l(s))$  be as defined in the previous section. Furthermore, let

$$\check{t}_l(s) = \frac{1}{l} (f(s; \check{t}_{l-1}(s)) + \check{t}_{l-1}(s) + \check{t}_{l-2}(s) + \dots + \check{t}_1(s)) \quad \text{for } l \leq l_{av};$$

and

$$\check{t}_l(s) = \frac{1}{l_{av}} (f(s; \check{t}_{l-1}(s)) + \check{t}_{l-1}(s) + \check{t}_{l-2}(s) + \dots + \check{t}_{l_{av}+1}(s)) \quad \text{for } l > l_{av}; \quad (26)$$

**Lemma 3.2.** *The sequence  $\check{t}_l(s)$  diverges for  $s > s^2$ , where  $s^2$  is threshold of the standard sum-product algorithm.*

The proof is given in Appendix A.2.

**Case 3:** Averaging strategies can be applied on probabilities directly, according to the rules described in the previous section. Proving that these techniques do not have thresholds larger than those of standard BP algorithms is technically more involved than proving the corresponding results for their LLR counterparts. Therefore, we first reformulate probabilistic averaging as a specialized form of LLR averaging, and then apply DE techniques to this case.

Observe first that

$$\tilde{t}_l(s) = \log \frac{\tilde{p}_l}{1 - \tilde{p}_l}$$

implies

$$\tilde{p}_l = \frac{e^{\tilde{t}_l(s)}}{1 + e^{\tilde{t}_l(s)}};$$

Define the probability  $p_l^f$  according to

$$\log \frac{p_l^f}{1 - p_l^f} = f(s; \log \frac{\tilde{p}_{l-1}}{1 - \tilde{p}_{l-1}}); \quad (27)$$

so that

$$p_l^f = \frac{e^{f(s; \log \frac{\tilde{p}_{l-1}}{1 - \tilde{p}_{l-1}})}}{1 + e^{f(s; \log \frac{\tilde{p}_{l-1}}{1 - \tilde{p}_{l-1}})}};$$

Averaging is performed in terms of computing the following geometric mean

$$\tilde{p}_l = \sqrt[l]{p_l^f \tilde{p}_{l-1} \tilde{p}_{l-2} \cdots \tilde{p}_{l_{av}+2}};$$

This form of probabilistic averaging is equivalent to averaging LLRs according to the formula

$$\tilde{t}_l(s) = \log \frac{\tilde{p}_l}{1 - \tilde{p}_l} = \log \frac{\sqrt[l]{p_l^f \tilde{p}_{l-1} \tilde{p}_{l-2} \cdots \tilde{p}_{l_{av}+2}}}{1 - \sqrt[l]{p_l^f \tilde{p}_{l-1} \tilde{p}_{l-2} \cdots \tilde{p}_{l_{av}+2}}} = \log \frac{\sqrt[l]{\frac{e^{f(s; \tilde{t}_{l-1}(s))}}{1 + e^{f(s; \tilde{t}_{l-1}(s))}} \frac{e^{\tilde{t}_{l-1}(s)}}{1 + e^{\tilde{t}_{l-1}(s)}} \cdots \frac{e^{\tilde{t}_{l_{av}+2}(s)}}{1 + e^{\tilde{t}_{l_{av}+2}(s)}}}}{\sqrt[l]{\frac{e^{f(s; \tilde{t}_{l-1}(s))}}{1 + e^{f(s; \tilde{t}_{l-1}(s))}} \frac{e^{\tilde{t}_{l-1}(s)}}{1 + e^{\tilde{t}_{l-1}(s)}} \cdots \frac{e^{\tilde{t}_{l_{av}+2}(s)}}{1 + e^{\tilde{t}_{l_{av}+2}(s)}}}}};$$

**Lemma 3.3.** *The sequence  $\tilde{t}_l(s)$  diverges for all  $s > s^*$ , where  $s^*$  denotes the threshold of the standard sum-product algorithm.*

The proof of the lemma is given in Appendix A.3.

We conclude this analysis by observing that the update equation for arithmetic averaged decoding of check probabilities is given by,

$$p_l^0 = \frac{1}{l_{av}} \left( \frac{e^{f(s; \frac{p_{l-1}^0}{1 - p_{l-1}^0})}}{1 + e^{f(s; \frac{p_{l-1}^0}{1 - p_{l-1}^0})}} + p_{l-1}^0 + p_{l-2}^0 + \cdots + p_{l_{av}+1}^0 \right); \quad (28)$$

and a similar proof for the invariance of the threshold of BP decoding can be performed for this case as well. The detailed proof is given in Appendix A.4.

### 3.4 The Influence of Averaging on Trapping Sets: Experimental Results

We provide next a comparative simulation study of the performance of the [2640;1320] Margulis code under BP and averaged BP decoding at an for SNR of 2.4 dB. At this SNR value, one can detect the onset of an error-floor and record the trapping sets that cause it. For a set of approximately 1.5 billion tested frames, 488 frames contained errors under standard BP decoding implemented as described in Section 2. Of these 488 frames, *all frames containing trapping sets* were successfully decoded using less than 200 iterations of arithmetic and geometric averaged decoding of variable node probabilities. Only frames that showed random-like oscillations in message values, and for which no erroneous message

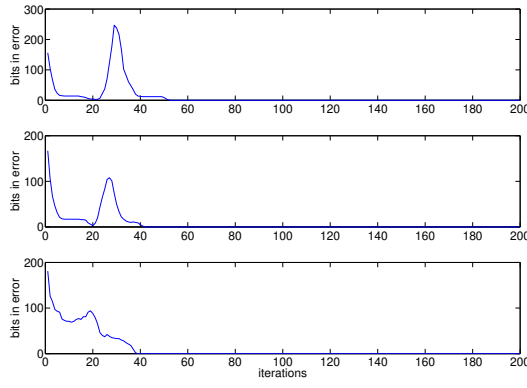


Figure 2: Frames with trapping set errors, averaged belief propagation.

trapping was observed<sup>6</sup>, were not corrected by averaging. Probabilistic averaging performed on check nodes resulted in almost the same performance, while averaging techniques applied to LLRs showed visibly inferior performance. We therefore focus on probabilistic averaging techniques for variable node messages only. Henceforth, we refer to the first set of described frames as *trapping frames*, and the second set of frames as *random frames*. We also tested the performance of the same averaged decoders on 36 million frames that were correctly decoded by standard BP algorithms. *All these tested frames* were correctly decoded under both forms of averaged decoding, for an appropriate setting of the parameters of the averaging algorithms. Consequently, averaging is not expected to change the performance of a decoder in the waterfall region of the BER curve, although in this regime it is not necessary to use this decoding strategy at all. Consider the data plotted in Figure 2, showing the changes in the number of erroneous variables with respect to the number of iterations during averaged belief propagation, for the same set of frames displayed in Figure 1. As can be seen, all three types of trapping sets were decoded without errors if message averaging was used.

The question of interest is, then, to explain why averaging eliminates the negative influence of trapping sets on the code graph. As described in the previous section, the success of averaging techniques can be attributed in part to the fact that they control chaotic behavior, eliminate unwanted oscillations, and combine expert opinions. To illustrate the influence of averaging on oscillation suppression in variable messages, consider the data listed below.

The data in the table pertains to a (14;4) trapping set. The first block (consisting of two rows) in each pair of blocks contains values of messages passed by one node in this set during standard BP. The second block contains the same messages under arithmetic (probability) averaged BP decoding. The symbol  $M$  is used to denote “method” and it refers to the parameters of arithmetic averaged decoders  $l_{\min}=l_{\text{av}}$ , as defined in the previous section. The symbol  $I$  is used to

---

<sup>6</sup>Very likely due to typical noise-configurations

M/I	1	2	3	4	5	6	7
1=1	0.9975	0.9995	0.9959	0.9947	0.9561	0.7212	0.4989
2=2	0.9975	0.9995	0.9977	0.9870	0.9810	0.9751	0.9586
M/I	8	9	10	11	12	13	14
1=1	<b>0.0061</b>	<b>0.9812</b>	0.9999	1.0000	1.0000	1.0000	1.0000
2=2	0.9284	0.8981	0.8752	0.8470	0.8203	0.7981	0.7977

Table 1: List of message values for standard and averaged BP.

describe the iteration index, ranging from one to 14. As one can see, the oscillations and progression rates of probability values observed during standard BP are significantly suppressed by averaging. One interesting example is printed in boldface letters, showing a change in message probability from 0.0061 to 0.9812 within one single iteration of standard BP decoding. The presence of such oscillations may be one of the reasons behind the fact that averaging reduces the error floor.

Another reason why averaging eliminates trapping events can be explained by its influence on the speed with which correct and incorrect estimates “flow” through the Tanner graph of the code. If the variables in a trapping set do not become significantly biased towards incorrect values at some early stage of decoding, there exists a high probability that they will converge to the correct estimates during a later stage of decoding. To investigate this phenomena more thoroughly, we propose to use specialized visualization methods for  $(12;4)$  and  $(14;4)$  trapping sets of the  $[2640;1320]$  Margulis code similar to those developed in [44, 11] for a different study. For reasons of clarity, we henceforth say that a variable node is *zero-biased* (*one-biased*), if the probability of this node having value zero exceeds (falls below) 0.5. A node is said to be *strongly* zero-biased, if the probability of the node having the value zero is close to one. Strongly one-biased is defined similarly. The above described probabilities can be *a priori* and *pseudoposterior* probabilities, depending on the iteration number.

Figure 8 shows the structure of a  $(14;4)$  trapping set of the  $[2640;1320]$  Margulis code as observed by a decoder that only has information about unsatisfied check nodes (represented by white squares). The figure depicts the basic  $(12;4)$  trapping set (gray circles), two “expansion” variables<sup>7</sup> (white circles), and the resulting  $(14;4)$  trapping set. This is the unique nesting structure for  $(12;4)$  and  $(14;4)$  trapping sets observed for all performed simulations, and first described in [5]. For ease of visualization, variable nodes are both “color coded” and “shape coded”. Blue circles are reserved for zero-biased variable nodes, while red circles are reserved for one-biased nodes. The radius  $r$  of a circle is proportional to the absolute value of the difference between the probability  $p$  of a variable being zero and the threshold 0.5. More

<sup>7</sup>Expansion variables will be investigated in more details in the next section.

precisely,  $r = \lfloor p - 0.5 \rfloor$ . Consequently, strongly biased variables are represented by circles of large radius. We refer to the four variables at the corners of the structure shown in figure 8 as the “outer ring”, and the four innermost corner variables (forming a square) as the “inner ring”. The Margulis code is a  $(3;6)$  regular code so that each check node has exactly six outgoing edges, of which only those connected to the trapping set variables are shown. With this restriction, the *degree of a check node within the trapping set* equals the number of its neighbors among the variables in the trapping set.

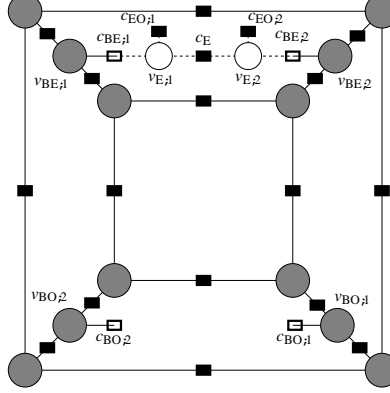


Figure 3: Structure of a basic  $(12,4)$  trapping set with expansion set (dashed), together forming a  $(14;4)$  trapping set.

Let us compare next the behavior of the standard BP decoder and the probability version of arithmetic averaging decoder with respect to the zero and one-biases of the variables. Figure 4 shows the a priori and seven pseudoposterior biases of variables in a  $(14;4)$  trapping set that were obtained by standard BP simulations, and are henceforth denoted by  $A$ . As can be seen, the majority of the variables in the trapping set exhibit a strong one-bias, and the few zero-biased variables tend to change their bias within a few consecutive iterations<sup>8</sup> After a certain number of iterations, all variables show a strong one-bias, although this bias is slightly smaller for the expansion compared to the basic trapping set variables. This bias persists for all subsequent iterations, which implies that the variable nodes exterior to the trapping set cannot change the decisions made by the trapping set variables. On the other hand, consider the same trapping set  $A$  and the same set of a priori biases with respect to averaged arithmetic decoding. Figure 5 depicts the evolution of the biases up to the number of iterations needed for correct decoding. One can observe a similar progression of biases as for standard BP, in the sense that at a certain iteration (in this case, iteration number 11) *all* variables in the trapping set have a one-bias. The strengths of the biases are, on average, significantly smaller for averaged then for standard BP decoding. Furthermore, the number of iterations needed for this event to occur is also significantly larger than for the case of standard decoding. This allows the variables exterior to the trapping set to revise the biases of the trapped

<sup>8</sup>This behavior is typical of all trapping sets detected during our simulations.

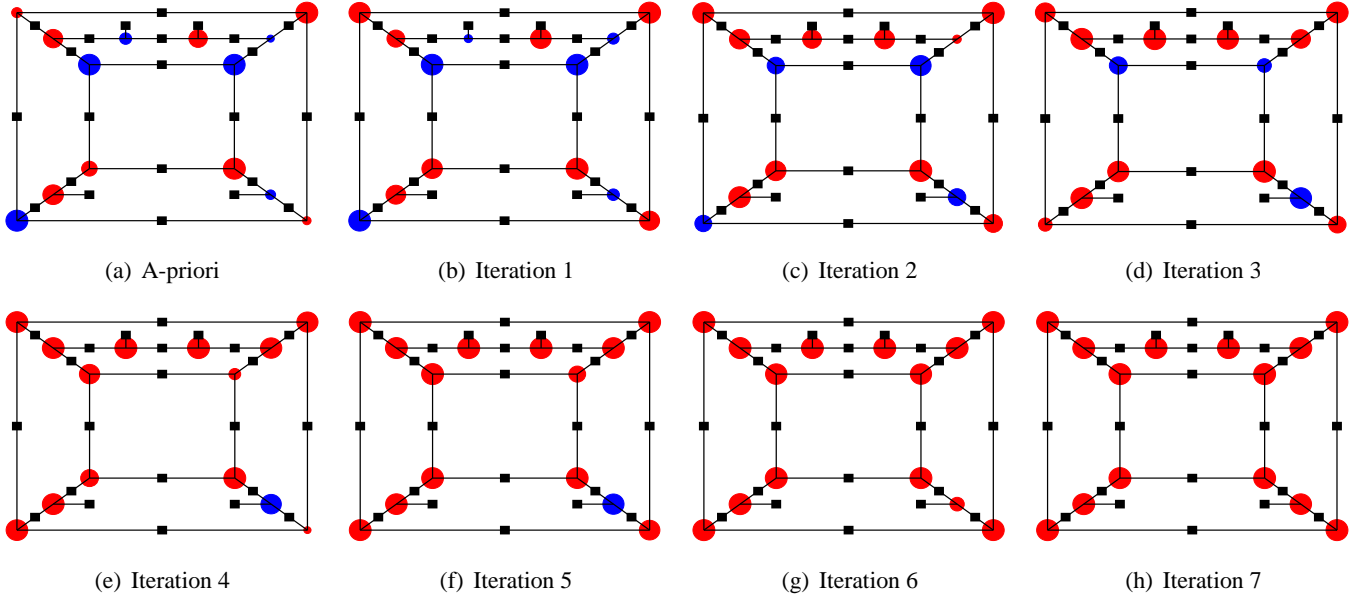


Figure 4: Visualization of the probabilities of the trapping set variables for standard belief propagation decoding of trapping set A during the first few iterations.

variables, which results in correct decoding after a sufficient number of additional iterations. These findings are typical of all the trapping sets investigated, and they are also present in the case of geometric averaging. Consequently, it can be deduced that averaging prevents potential problems in the decoding process by reducing the magnitude of large biases, and slowing down the changes in biases of variable nodes.

frame #	Method								frame #	$\theta = 0.05$	$\theta = 0.1$	$\theta = 0.2$
	2/2	5/2	6/2	7/2	8/2	2/3	5/3	7/3		2/2		
1	22	23	32	40	43	36	34	54	1	22	23	23
2	21	16	35	41	44	33	22	57	2	21	21	21
3	19	19	29	37	40	28	29	47	3	20	19	20
4	20	21	23	37	41	32	29	49	4	21	20	20
5	23	20	18	38	42	35	26	48	5	24	23	24
6	24	20	18	24	42	34	26	25	6	24	24	23
7	20	24	34	39	41	30	35	53	7	20	20	20
8	21	24	33	40	42	33	34	53	8	21	21	21
9	26	26	28	36	43	44	40	48	9	26	25	24
10	25	24	38	42	44	40	39	58	10	25	25	24

Table 2: Convergence speed of averaged decoding.

The number of overall iterations of averaged decoding is usually larger than the average number of iterations needed for standard belief propagation decoding of frames that do not exhibit point trapping set behavior. The reader is referred to Table 2 for a more precise count of this number of iterations for arithmetic averaged BP decoding. In addition, Table 3

lists the average number of iterations needed for error-free decoding of 1000 frames by standard and averaged belief propagation. It can be observed that the later the averaging process is started (i.e., the larger the value  $l_{\min}$ ), the smaller the expected number of iterations required for successful averaged decoding. Consequently, one needs to choose the parameters  $l_{\min}$  and  $l_{av}$  in a judicious manner that will ensure sufficiently fast and correct progression of the biases of variables outside the trapping set, while at the same time slow down erroneous messages reaching the trapping sets.

The performance of the adaptive averaging scheme with parameter  $\theta$  is shown Table 2. The operational parameters of the averaged decoding algorithm are again given by the pair of values  $l_{\min}=l_{av}$ .

As can be seen from Tables 2 and 3, the best results in terms of decoding complexity can be achieved for the 2=2 and 5=2 arithmetic averaging method. Adaptive averaging does not seem to offer any advantages compared to general averaging methods in terms of error-rate performance.

Method (1000 frames)	BP	2/2	6/2	7/2
Average # of iterations	7.4	11.22	14.14	10.43

Table 3: Convergence speed of averaged decoding for correctly decoded frames.

### 3.5 Geometric versus Arithmetic Averaging

We compare next geometric and arithmetic averaging techniques applied to variable nodes. We point out once again that averaging of LLRs showed inferior results compared to its probability-based counterparts, and we again focus on averaging techniques operating on probabilities of variable node messages. The decoder parameters are, again, two integers  $(l_{\min}; l_{av})$ , describing the starting iterations for averaging  $l_{\min}$ , and the number of iterations  $l_{av}$  over which averaging is performed. Arithmetic averaging follows the update rules listed in Equation (16), while geometric averaging is performed according to Equation (17). A total number of 47 point trapping were tested with respect to these two averaging techniques. Table 4 shows the average number of iterations required for error-free decoding of arithmetic and geometric averaged decoders, as well as the maximum number of iterations for the 47 frames. Note that the maximum number of iterations was set to 200. Obviously, for all the cases listed, the required number of iterations for averaging over  $l_{av} = 1$  iterations is 200, since this case corresponds to standard BP.

Geometric averaging is extremely sensitive to the particular choice of the decoder parameters  $(l_{\min}; l_{av})$ . If more than two iterations are used and if averaging is initiated after nine or more iterations, certain numerical problems are encountered that prevent the decoder to converge to a meaningful solution.

Nevertheless, the results listed in the table also indicate that geometric averaging with the best set of decoder pa-

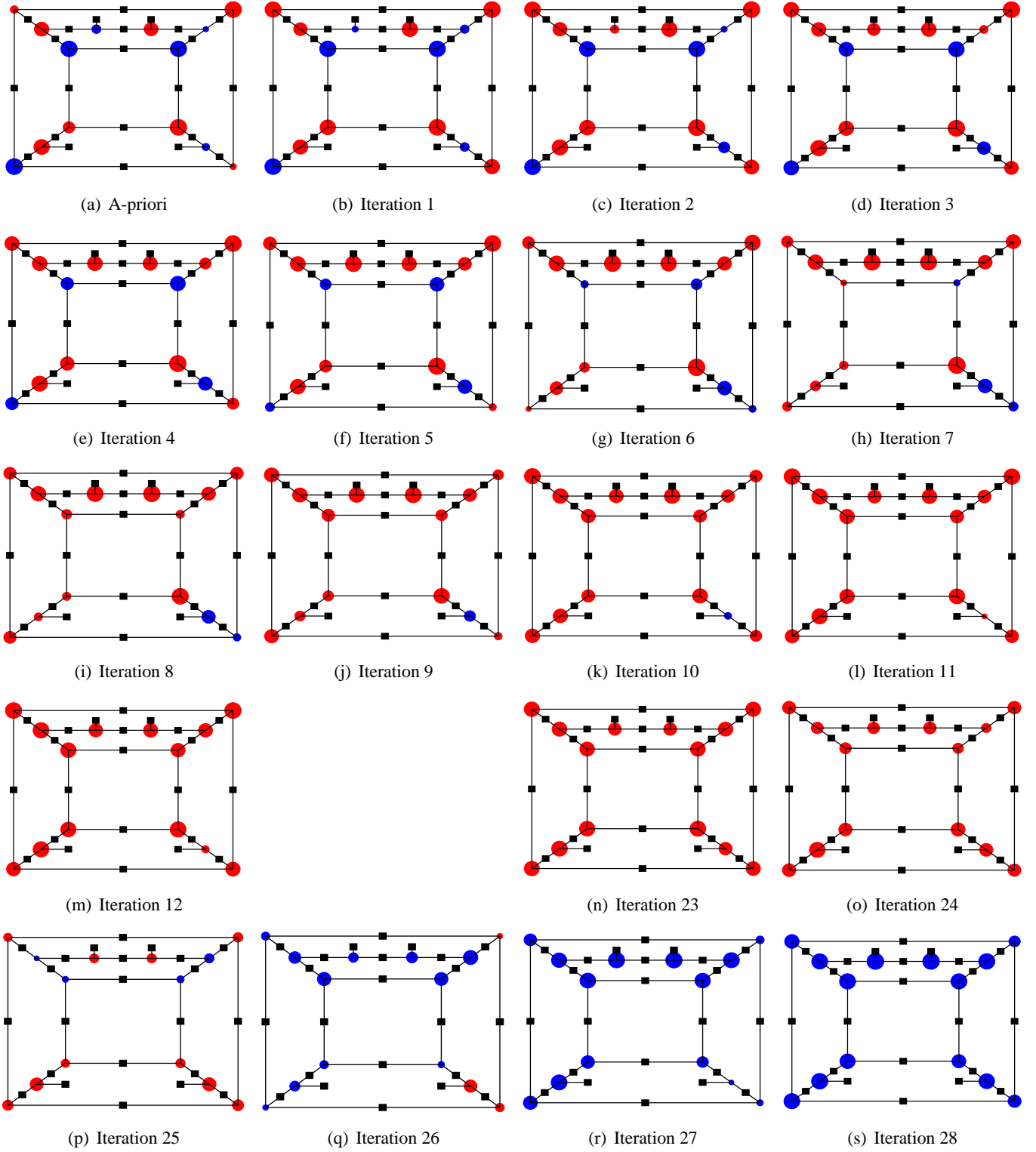


Figure 5: Visualization of the probabilities of the trapping set variables for averaged BP decoding using arithmetic averaging of probabilities of trapping set A.

rameters can decode the same number of errors as arithmetic averaging with its optimal set of parameters. Furthermore, geometric averaging results in faster biasing rates compared to arithmetic averaging.



$l_{\min}$ $n$ $l_{\text{av}}$	Average number of averaged decoding iterations							
	arithmetic				geometric			
	2	3	4	5	2	3	4	5
1	22.7	36.9	57.8	85.7	20.6	30.8	46.1	66.7
2	21.8	33.8	51.2	74.4	19.7	27.8	39.9	55.6
3	20.9	31.2	45.8	65.1	19.2	25.3	34.4	46.1
4	20.3	29.5	42.5	59.2	19.7	24.0	31.6	40.4
5	20.7	29.7	41.0	55.5	22.0	27.1	35.2	44.8

Table 4: Average number of iterations necessary for correct decoding of point trapping sets using arithmetic and geometric averaging. Averaging starts after iteration  $l_{\min}$ , average taken over  $l_{\text{av}}$  iterations.

The BER performance of standard BP decoding is compared to averaged decoding techniques in Figure 6. As all trapping frames that were decoded without errors by the arithmetic averaging decoder were also decoded without errors by geometric averaging decoders, only one curve is displayed for both these methods. Note that averaging is only used in the error floor region (i.e. only once a certain SNR is reached). The curves in Figure 6 are generated using averaged decoding that starts at the first iteration,  $l_{\min} = 1$ , and performs averaging over  $l_{\text{av}} = 2; 3; \text{and } 4$  iterations.

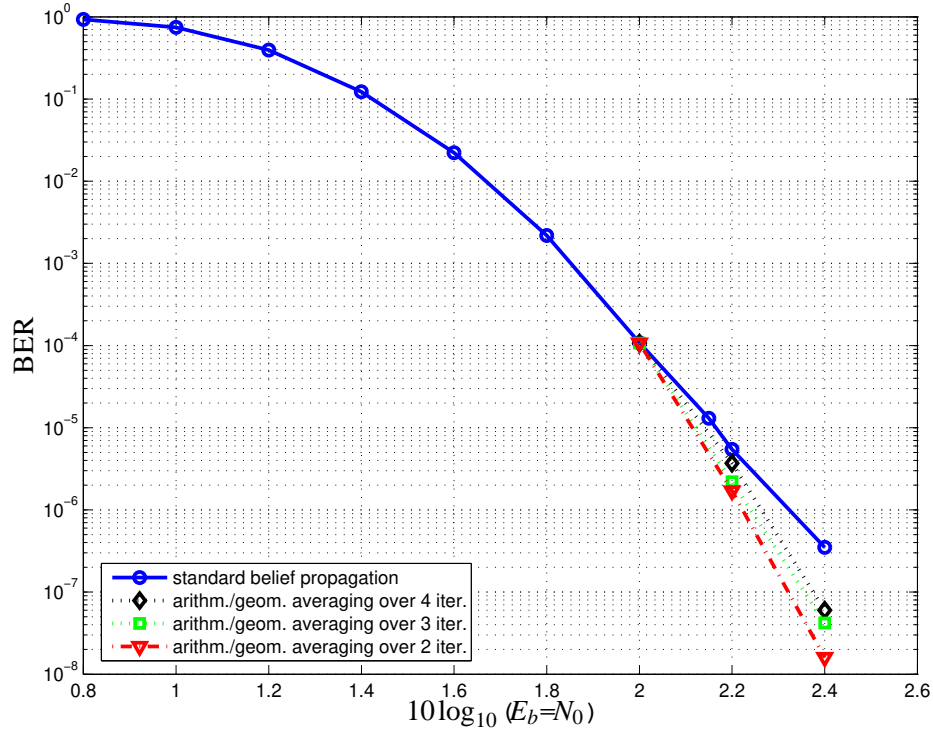


Figure 6: Performance comparison: standard belief propagation decoding versus averaged decoding starting with  $l_{\min} = 1$ ,  $l_{\text{av}} = 2; 3; 4$ .

Averaged decoders with  $l_{\text{av}} = 2$  show the best results in terms of performance.

**Remark:** We also implemented averaged decoders that use Nörlund-type of averaging. Here, the update rules for the

probabilities  $\hat{p}_l$ , and their sums  $s_j = \sum_{i=0}^j \hat{p}_i$ , were chosen as

$$\begin{aligned}
\hat{p}_l &= \frac{\beta_l s_1 + \beta_{l-1} s_2 + \dots + \beta_{l-k+1} s_k + \dots + \beta_1 s_l}{\beta_1 + \beta_2 + \dots + \beta_l} \\
&= \frac{\beta_l \hat{p}_1 + \beta_{l-1} (\hat{p}_1 + \hat{p}_2) + \dots + \beta_{l-k+1} \sum_{i=1}^k \hat{p}_i + \dots + \beta_1 \sum_{i=1}^l \hat{p}_i}{\beta_1 + \beta_2 + \dots + \beta_l} \\
&= \frac{\hat{p}_1 \sum_{i=1}^l \beta_i + \hat{p}_2 \sum_{i=1}^{l-1} \beta_i + \dots + \hat{p}_k \sum_{i=1}^{l-k+1} \beta_i + \dots + \hat{p}_l \beta_1}{\sum_{i=1}^l \beta_i}
\end{aligned} \tag{29}$$

As is the case for geometric averaging, Nörlund-type of averaging is very sensitive to the particular choice of decoding parameters - in this case, the parameters  $\beta_i$  included. For example, by letting the sequence  $\beta_i; i = 1; \dots; l_{av}$  be  $(l=l)^r; (l-1=l)^r; \dots; (1=l)^r; (1=l)^r$  we obtained decoders that actually tend to spread errors outside trapping sets, rather than eliminate them. In most cases, a (12;4) or (14;4) trapping set resulted in 120 - 160 errors upon termination of the decoding process (i.e. after 200 iterations). A much better performance was obtained for a sequence of  $\beta_i$ 's of the form  $1=(1!); 1=(2!); 1=(3!); 1=(4!); \dots$ , although even in this case this averaging technique was inferior in performance compared to arithmetic and geometric averaging.

## 4 Trapping Sets and Redundant Parity-Check Equations

An alternative approach for reducing error floors of LDPC codes consists in choosing an appropriate redundant parity-check matrix for decoding, rather than altering the decoding algorithm itself. For that purpose, let us assume that during decoding on the standard Tanner graph of the Margulis code, a frame is encountered with errors confined to a (12;4) trapping set. The problem of interest is to investigate how the estimated values of these 12 trapping set variables change with the addition of one or more redundant parity-check equations. If these redundant check nodes increase the number of unsatisfied checks in a trapping set with 12 variables from four to five, is the decoder still going to make an erroneous decision? For a given number of variables, how many unsatisfied checks are needed in order for the decoder to recognize errors confined to a trapping set and to correct them? These questions are addressed in this section, and our results show that increasing the number of unsatisfied checks connected to trapping sets of a code in terms of adding redundant parity-check equations leads (with high probability) to correct decoding of most trapped frames. More precisely, we show that for the [2640;1320] Margulis code, errors confined to point trapping sets can be completely eliminated by adding *only one redundant row* to the standard parity-check matrix of the code.

Figure 7 illustrates the effect that one redundant row in the parity-check matrix of a code can exhibit on the performance of the BP algorithm. Figure 7(a) shows the behavior of the iterative decoder when used over the standard Tanner

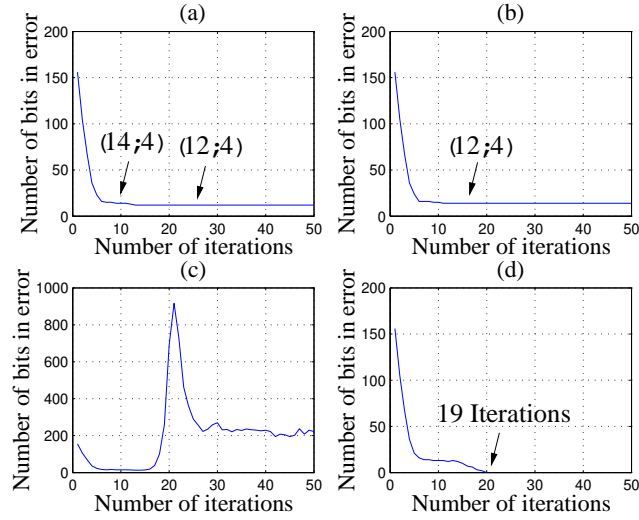


Figure 7: Number of bits in error for no additional parity-check (a) and different parity-checks appended (b, c, d)

graph of the Margulis code. The decoder first gets trapped in a  $(14;4)$  trapping set, and then settles in its unique  $(12;4)$  trapping subset. Once a trapping event is detected, an appropriately chosen parity-check equation can be appended to the matrix and the decoding process can be restarted. Figures 7(b) and 7(c) show the performance of the decoder when one such redundant row is added to the parity-check matrix in a way that the projection of the 12 trapped variables confined to this row has weight one. In Figure 7(b) the decoder gets trapped in the  $(14;4)$  trapping set already observed in Figure 7(a), since the projection of its 14 variables on the redundant row has weight two, and the erroneous variables inside the  $(14;4)$  trapping set are even more biased towards an incorrect decision. The additional parity-check equation used in Figure 7(c) has row-weight one when confined to both the  $(12;4)$  as well as the  $(14;4)$  trapping set. Nevertheless, it does not lead to successful decoding but rather results in the decoder being trapped in an aperiodic trapping set. In Figure 7(d), the output of the decoder for another choice of a redundant parity-check equation with projection of weight one confined to both the  $(12;4)$  as well as the  $(14;4)$  trapping set is shown. In this case, the decoder successfully identifies the codeword after only 19 iterations. Note that in all these experiments, the channel noise realizations were the same.

As can be seen from the example above, the output of the decoder operating on the augmented Tanner graph depends on the effect of the redundant row on the  $(12;4)$  trapping set. If the projection of the 12 columns on the redundant parity-check equation results in a row of weight 1, the  $(12;4)$  trapping set is converted into an elementary  $(12;5)$  trapping set. Such a set has one more unsatisfied check equation, which may help the decoder in identifying some erroneous variables. Unfortunately, the expansion of a  $(12;4)$  trapping set into a  $(12;5)$  set often does not lead to a correctly decoded frame, but rather forces the decoder into a  $(14;4)$  trapping set containing the original  $(12;4)$  trapping set. If,

on the other hand, both the projections of the underlying 12 and the extended 14 trapping set variables result in rows of weight one corresponding to the redundant parity-check equation, the decoder converges with high probability to the correct codeword. For all  $(12;4)$  and  $(14;4)$  trapping sets investigated, a *single parity-check equation* can be identified that can simultaneously increase the number of unsatisfied checks in the  $(12;4)$  and their extended  $(14;4)$  trapping sets. More precisely, in all such cases, the projections of both the 12 and the 14 variables contained a vector of weight one when confined to the redundant row.

Parity-check equations that lead to this effect can be found by using two different approaches. One approach, termed *genie-aided search*, assumes the knowledge of the erroneous trapping variables. Since such knowledge is not readily available during decoding, another approach, termed *structured search*, is proposed as well. The structured approach provides for simple and computationally inexpensive identification of appropriate redundant parity checks to be used for decoding trapping errors, but it requires some prior knowledge on the structure of trapping sets encountered during decoding.

#### 4.1 Genie-aided random search

This method is primarily used to demonstrate the ease with which a parity-check equation with projections of weight one on both the 12 and 14 trapping set variables can be found. Observe that the existence of such an equation is a consequence of the fact that the Margulis code has minimum distance not smaller than 40 and that the codewords of its dual code consequently form an orthogonal array of strength at least 40 [45] (we will revisit the properties of a code in terms of its defining orthogonal array in Section 4.4). The genie-aided search algorithm can be summarized as follows:

- 1: List all parity-check equations involving the variable nodes of a  $(12;4)$  trapping set.
- 2: Form all linear combinations of the equations found in step 1.
- 3: Find linear combinations that have weight one when projected to both the  $(12;4)$  and  $(14;4)$  trapping set variables.
- 4: Append in succession each of these parity-check equations to the standard parity-check matrix and check if the decoder converges to a correct codeword.

In all investigated cases, the redundant rows found during the search were not previously present in the standard parity-check matrix, as can be easily determined based on its weight: while all parity-checks of the original parity-check matrix have weight 6, the weight of the appended rows was found to be an even number in the range from 18 to 50.

## 4.2 Structured search

We describe next an approach for identifying good candidates for redundant parity-checks without using side information regarding the position of erroneous variables, but rather by exploiting structural properties of the  $(12;4)$  and  $(14;4)$  trapping sets in the  $[2640;1320]$  Margulis code.

Throughout the remainder of this section, we call the variables and checks introduced by extending a  $(12;4)$  to a  $(14;4)$  trapping set *expansion variables* and *expansion checks*, respectively. The notation B, E, and O is used to refer to the basic  $(12;4)$  trapping set, its expansion variables and checks, and the graph outside (i.e. complementary to) the  $(14;4)$  trapping set, respectively. Since the Margulis code is regular, with variable node degree  $d_v = 3$  and check node degree  $d_c = 6$ , an elementary  $(a;b)$  trapping set with  $a$  variables and  $b$  check nodes of degree one<sup>9</sup> has a fixed number of checks. Therefore, in order to extend an elementary  $(12;4)$  trapping set to a  $(14;4)$  trapping set, two variables and three checks have to be added. The notions of basic, expansion and outside variables and check nodes are illustrated in Figure 3.

Since the Margulis code has no four-cycles, at most one expansion check can be connected to both the expansion variables. Consequently, either three or four edges emanating from the expansion variables are connected to expansion check nodes, while the remaining edges are connected to check nodes whose degree in the basic  $(12;4)$  trapping set is one. Thus there exist only two possible configurations for such trapping sets, as shown in Figure 8:

1. Based only on the knowledge of check nodes of degree one within the basic  $(12;4)$  trapping set, it is straightforward to determine the whole expansion set: the two degree-one checks of the basic  $(12;4)$  trapping set are connected through two variable nodes to one additional check node. These two variable nodes are the expansion variables.
2. In the second configuration, the expansion variables do not share a check node.

All frames we observed during our simulations correspond to configurations of the first type.

For configuration 1, denote the two expansion variables by  $v_{E;1}$  and  $v_{E;2}$ . Furthermore, denote the check node connected to both these variables by  $c_E$ . The unsatisfied check nodes in the basic trapping set neighboring the expansion variables are denoted by  $c_{BE;1}$  and  $c_{BE;2}$ , while the variable nodes in the basic trapping set connected to check nodes  $c_{BE;1}$  and  $c_{BE;2}$  are denoted by  $v_{BE;1}$  and  $v_{BE;2}$ , respectively. The check nodes of degree one in the expansion of the trapping set are  $c_{EO;1}$  and  $c_{EO;2}$ . The two remaining check nodes of degree one in the basic trapping set are termed  $c_{BO;1}$  and

---

<sup>9</sup>These check nodes, incidentally, correspond to unsatisfied check nodes, that can be readily identified.

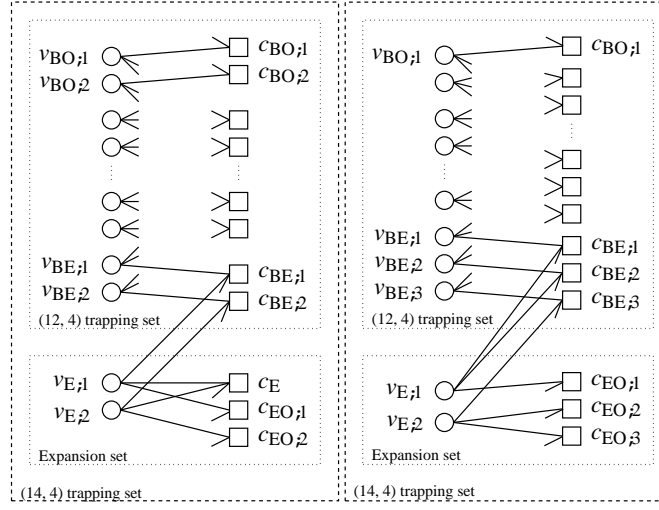


Figure 8: Trapping set structure of a (12;4) trapping set and its expansion. (a) configuration 1, (b) configuration 2.

$c_{BO,2}$ , and the variable nodes within the basic (12;4) trapping set connected to them  $v_{BO,1}$  and  $v_{BO,2}$ , respectively (see Figure 8(a)). The configuration involving all the aforementioned checks and variables is illustrated in Table 5.

	Expansion Variables		Basic Trapping Set Variables			
	$v_{E,1}$	$v_{E,2}$	$v_{BE,1}$	$v_{BE,2}$	$v_{BO,1}$	$v_{BO,2}$
$c_E$	1	1	0	0	0	0
$c_{EO,1}$	1	0	0	0	0	0
$c_{EO,2}$	0	1	0	0	0	0
$c_{BE,1}$	1	0	1	0	0	0
$c_{BE,2}$	0	1	0	1	0	0
$c_{BO,1}$	0	0	0	0	1	0
$c_{BO,2}$	0	0	0	0	0	1

Table 5: Projection of the basic trapping set and the expansion variables

The parity-check equations containing the projections described in Table 5 can be linearly combined to generate a redundant parity-check equation that has a projection of odd weight in both the (12;4) and the (14;4) trapping set. There are three different methods for linearly combining the parity-check equations with projections as shown in Table 5.

Method  $S_1$  refers to adding the rows indexed by  $(c_E, c_{EO,1}, c_{BE,2})$ ,  $(c_E, c_{EO,2}, c_{BE,1})$ ,  $(c_{EO,1}, c_{BE,1})$ , and  $(c_{EO,2}, c_{BE,2})$ . Observe that all these combinations have a projection of weight one within the basic trapping set. Method  $S_2$  refers to adding the rows indexed by  $(c_E, c_{EO,1})$  and  $(c_E, c_{EO,2})$ . Observe that all these combinations have a projection of weight one within the expansion variables. Method  $S_3$  differs from the previous methods in so far that it may generate redundant parity-check equations with odd-weight projections that are not necessarily of weight one. Candidate equations are obtained by adding the rows indexed by  $(c_E, c_{BO,1})$ ,  $(c_E, c_{BO,2})$ ,  $(c_E, c_{BE,1}, c_{BE,2}, c_{BO,1})$ ,  $(c_E, c_{BE,1}, c_{BE,2}, c_{BO,2})$ ,  $(c_{BO,1},$

$c_{BO,2}$ ,  $c_{EO,1}$ ,  $c_{BE,2}$ ), and  $(c_{BO,1}, c_{BO,2}, c_{EO,2}, c_{BE,1})$ . The Hamming weight of the constructed rows is an even integer between 10 and 24. The lower bound 10 is met by the constructions  $S_1$  and  $S_2$  if the supports of two added parity-checks share exactly one element. The intersection of the supports cannot have more than one element, since the code has no four cycles. Method  $S_3$  meets the upper bound 24: four parity-check equations are added and none of the variables listed in Table 5 occur in the support of more than one parity-check.

If a trapping set of the form shown in Figure 8(b) is present in the code graph, then the two expansion variables cannot have a common check node. Consequently, the expansion variable  $v_{E,1}$  is connected to two of the degree-one check nodes of the basic trapping set.<sup>10</sup> If there is only one variable node connected to two degree-one checks, denoted by  $c_{BE,1}$  and  $c_{BE,2}$ , the variable of interest is the expansion variable  $v_{E,1}$ , which is also connected to expansion check node  $c_{EO,1}$ . Observe that the expansion variable  $v_{E,2}$  is strongly influenced by its two neighboring check nodes connected to the outside graph and it cannot be uniquely determined. Due to this limited knowledge of the expansion set, there are two possible ways to generate a redundant parity-check with an odd projection weight on the basic trapping set, involving the sums of the rows  $(c_{EO,1}, c_{BE,1})$  as well as  $(c_{EO,1}, c_{BE,2})$ . A similar analysis can be conducted for  $(14;4)$  trapping sets. Details regarding this procedure are omitted.

Table 6 illustrates the application of methods  $S_1$ ,  $S_2$ , and  $S_3$ , as well as the genie-aided random search for identifying redundant parity-check equations that lead to correct decoding of all frames erroneously decoded on the standard Tanner graph (described in the previous section). For illustration purposes, we focus on 15 frames chosen from this category. The table includes data describing the parameters of the sets in which the decoder was initially trapped, the number of parity-check equations that had to be added in order to generate the redundant equation used in the genie-aided random search method, and the number of iterations performed by the decoder until successful decoding. Also listed are the types of structured methods used to generate the redundant parity-check equation. Underlined symbols refer to methods that used the minimum number of iterations to converge to the correct solution. This number is also shown in the rightmost column of the table.

Although decoding with a redundant parity-check matrix should, in principle, only be performed in the error-floor region (by restarting the decoder if it gets “trapped”), simulation results indicate that the performance in the waterfall region is not influenced by the presence of one redundant parity-check, so that decoding can be performed with the redundant parity-check matrix for all SNR values.

---

<sup>10</sup>One must keep in mind that the choice for such a variable may not be unique.

Genie-aided random search, 4.1				Structured search, 4.2	
Frame	Type	# of comb. parity-checks	Requ. iterations	Working structured search methods	Requ. iterations
1	(12;4)	4	24	$S_1, \underline{S_3}$	16
2	(12;4)	9	22	$S_1, \underline{S_2}$	22
4	(12;4)	6	24	$\underline{S_3}$	36
5	(12;4)	12	28	$\underline{S_3}$	25
6	(14;4)	7	27	$S_1, \underline{S_3}$	20
7	(12;4)	4	20	$\underline{S_1}, S_2, S_3$	13
8	(14;4)	9	18	$\underline{S_3}$	17
9	(12;4)	5	20	$\underline{S_1}$	24
10	(12;4)	4	22	$\underline{S_3}$	17
11	(14;4)	5	18	$\underline{S_3}$	14
12	(12;4)	8	21	$\underline{S_1}$	27
13	(12;4)	4	19	$\underline{S_1}, S_2, S_3$	16
14	(12;4)	5	26	$\underline{S_3}$	16
15	(14;4)	6	24	$\underline{S_1}$	26
16	(12;4)	5	21	$\underline{S_3}$	16

Table 6: Summary of simulation results for processed frames using the genie-aided random search and structured search methods. The software used to generate part of the results is available upon request from the authors.

### 4.3 Redundancy and Variable Node Biases

Intuitively, it is clear that adding properly selected redundant check nodes can change the flux of “correct” messages to and from variable nodes within the trapping set. How exactly this information is passed and how it influences the evolution of biases of variables in the trapping is described next.

For this purpose, we start by considering redundant parity-check equations in the decoding matrix that increase the number of odd-degree checks in the Tanner graph of *all* nested trapping sets. Note that one parity-check equation may increase the number of *odd-degree* checks in one trapping set, but simultaneously increase the number of *even-degree* checks in another set containing that given trapping set. Determining when such an event occurs is very hard, and largely dependent on the structure of the Tanner graph of the code. Consequently, we focus on only one redundant parity-check equation simultaneously altering only two nested trapping sets, which is the case for the already described (12;4) and (14;4) trapping sets. An illustrative example that does not involve these two trapping sets is given in Figure 9. It shows three instances of belief propagation decoding involving three different parity-check matrices: the solid line is used to represent the standard parity-check matrix, the dashed line corresponds to a parity-check matrix with one redundant equation, while the dash-dotted line follows the decoding process on the standard matrix augmented with seven redundant rows. For the standard parity-check matrix, the decoder gets trapped in a (12;4) set. When one more parity-check is added, the decoder produces errors confined to a (14;4) set. This one line increases the number of odd-degree checks in



the  $(12;4)$ , and, at the same time, the number of even-degree checks in the  $(14;4)$  set. Adding six more equations leads to an aperiodic trapping frame, which visits a  $(18;12)$  trapping set in the span of two iterations.

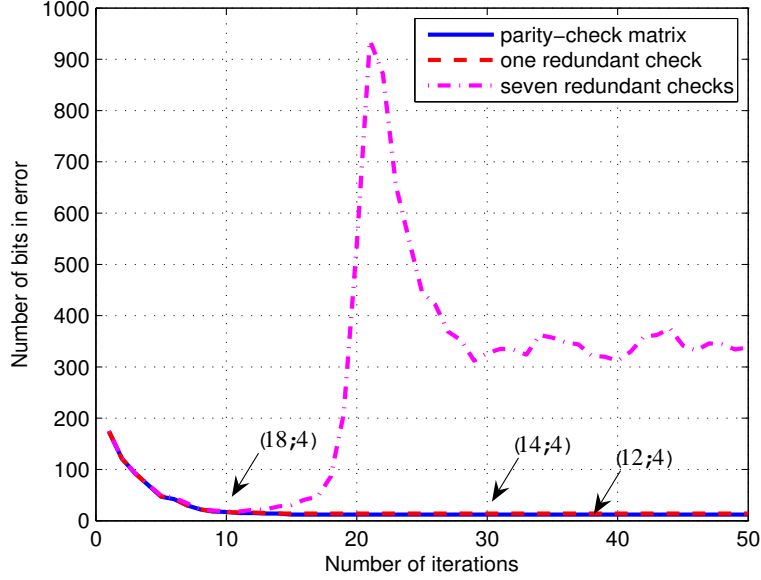


Figure 9: The influence of redundant parity-check equations on a frame with a  $(12;4)$  trapping set.

The zero- and one-biases of variables in two trapping sets, denoted by  $B$  and  $C$ , and augmented in several different ways, are depicted in Figure 10 and Figure 11. The redundant parity-check equations are generated in terms of the structured search methods described in Section 4. Method  $S_1$  results in converting both the  $(12;4)$  and  $(14;4)$  trapping sets into  $(12;5)$  and  $(14;5)$  trapping sets (e.g. Fig. 10(b)), while method  $S_2$  only alters the number of odd-degree checks in the  $(14;4)$  trapping set (e.g. Fig. 10(c)). Method  $S_3$  results in the formation of a non-elementary trapping set. The resulting structures are shown for the trapping set  $B$  in Figure 10. We choose to display both those configurations that are correctly decoded, as well as those that are not correctly decoded, in order to identify the underlying interactions between the redundant check and the variable nodes with zero- and one-biases. Nodes connected by thin dotted lines do not belong to the set of erroneously decoded variables. The redundant check nodes are emphasized by using thick dotted lines for their edges and are pointed to by arrows.

Figure 10(a) shows the structure of trapping set  $B$  with a redundant row obtained by adding the check equations  $c_E - c_{EO;1} - c_{BE;2}$ . The addition of such a degree-one check equation does not result in correct decoding. The only two redundant parity-checks leading to successful decoding of the  $(12;4)$  trapping set are obtained by adding check equations  $c_E - c_{EO;1} - c_{BE;2}$  (Figure 10(b)), and  $c_E - c_{EO;2}$  (Figure 10(c)), respectively. The inclusion of the former check equation

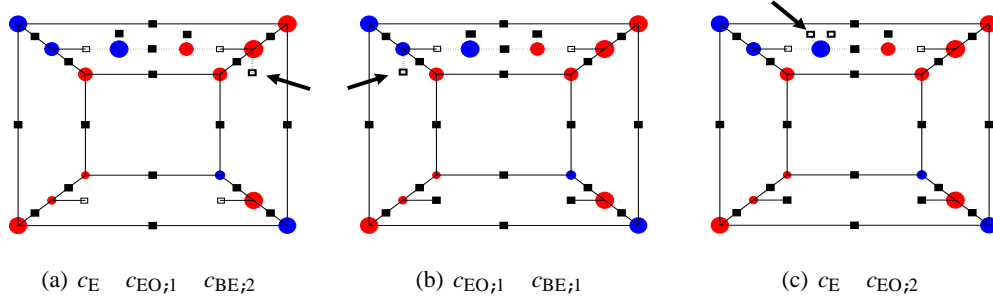


Figure 10: A-priori probabilities and trapping set structure for different redundant checks, frame B

results in an increase of the number of odd-degree checks in the  $(12;4)$  basic trapping set, as well as in the extended  $(14;4)$  trapping set. The latter check only modifies the structure of the  $(14;4)$  trapping set, since it is connected to the expansion set variables. Despite the fact that these two redundant equations lead to different overall changes in the trapping set structures, one of their common features is that they both connect a zero-biased trapping set variable with a variable outside the trapping set, and therefore provide this variable with relevant information needed for correct decoding.

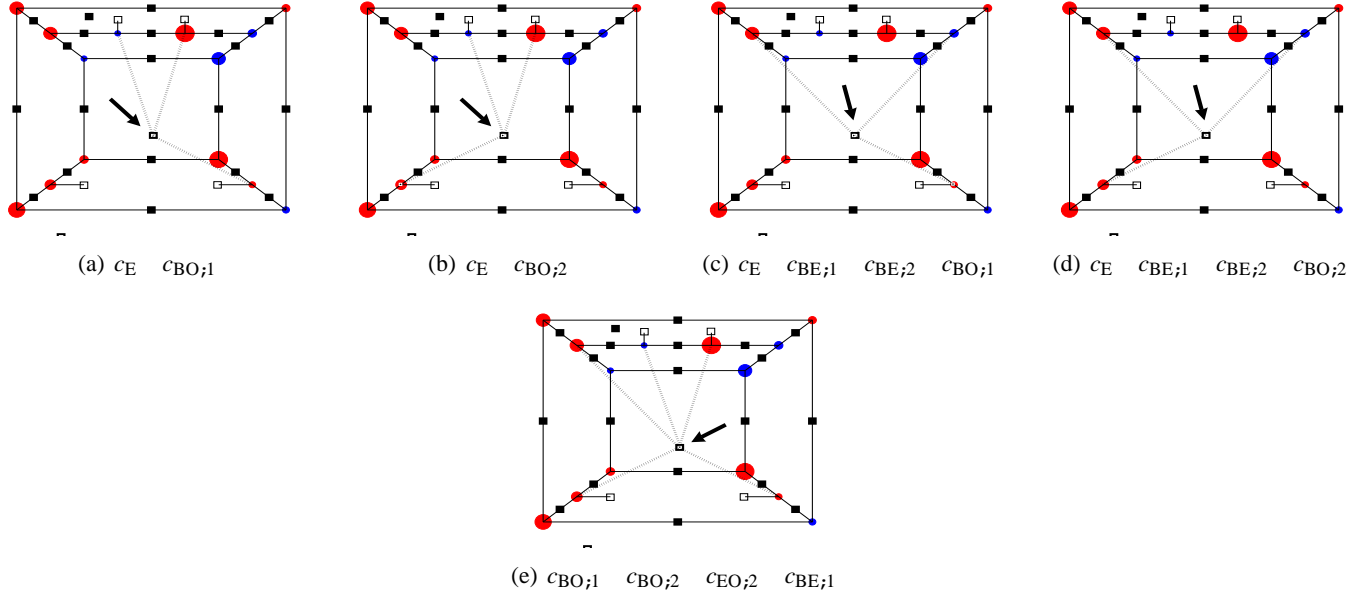


Figure 11: A-priori probabilities and trapping set structure for different redundant checks, trapping set C

The modified trapping set structure displayed in Figure 10(b) can be constructed from two different redundant check equations,  $c_{EO;1} \ c_{BE;2}$  and  $c_E \ c_{EO;2} \ c_{BE;1}$ , respectively, while only the former check equation results in error-free decoding. This indicates that the success of decoding using redundant check equations not only depends on the bias of the variable node the redundant check is connected to, but also on the bias of the variables neighboring a redundant check. As it would seem intuitive that the connection of a redundant check to a variable in the trapping set supports

this variable in developing or maintaining a zero-bias, the decoding process appears to be of a more complex nature. Successful decoding of trapping sets using redundant check equations depends also on the biases of all the trapping set variables and their neighboring nodes.

The redundant checks leading to successful decoding of trapping set  $C$  are depicted in Figure 11. Observe that adding these redundant checks from method  $S3$  makes the  $(14;4)$  trapping set non-elementary and introduces additional cycles within the trapping set. The redundant checks displayed in Figures 11(a), 11(b), and 11(e), respectively, also connect the expansion set variables, therefore forming a four-cycle and reducing the girth of the Tanner graph. It has to be noted that for all tested frames, the redundant equations obtained by method  $S3$  resulted in the best decoder performance.

Contrary to averaged BP decoding, which slows down the convergence of the bias of the variable nodes, redundant parity-check equations show, if at all, only a very limited influence on the speed of convergence. For most redundant check equations that resulted in a correctly decoded frame, variable nodes of the trapping set were strongly one-biased after several iterations. At a later stage of the decoding process, these biases were reverted. There is, however, no one single set of parameters capable of describing the connection between the structure of a redundant check, the initial bias of the trapping set variables, and the probability of successfully decoding a frame. Furthermore, strongly biased nodes sometimes cause numerical instabilities in the decoding algorithm, making the decoding process highly unpredictable. As a final remark, we point out that the location of the non-zero entry within the projection of the redundant parity-check equation on the  $(12;4)$  or  $(14;4)$  trapping set does not seem to influence the performance of the decoder.

#### 4.4 Redundancy Versus Trapping Set Size: An Analytical Study

In what follows, we investigate the fundamental theoretical trade-offs between the number of rows in a parity-check matrix of a code and the size of its smallest trapping set from a given class. For all our subsequent derivations, we need the following definition.

**Definition 4.1.** ([45, p.5]) An orthogonal array of strength  $t$  is an array of dimensions  $m \times n$  such that every  $m \times t$  subarray contains *each* possible  $t$ -tuple *the same number of times*. The codewords of a  $[n; k; d]$  code  $C$  form an orthogonal array of dimension  $2^k \times n$  of strength  $d^2 - 1$ , where  $d^2$  denotes the dual distance of  $C$ .

Let  $T_H(a; b)$  denote the number of trapping sets in the parity-check matrix  $H$  with parameters  $(a; b)$ . We have the following result regarding  $T_H(a; b)$  for a matrix  $H$  that consists of all codewords of the dual code.

**Proposition 4.1.** *Let  $H$  consist of all  $2^{n-k}$  codewords of the dual of an  $[n;k;d]$  code  $C$ , for which  $n-k \geq 1$ . Then  $T_H(a;b) = 0$  for all  $a$  and  $b$  such that  $1 \leq a \leq d-1$ , and  $b \notin 2^{n-k-1}$ .*

Proposition 4.1 shows that a parity-check matrix that consists of all codewords of the dual code cannot contain trapping sets with  $1 \leq a \leq d-1$  variables that have fewer than  $2^{n-k-1}$  checks connected to them an odd number of times. This is a direct consequence of the fact that  $H$  in this case represents an orthogonal array, so that each set of  $1 \leq a \leq d-1$  columns of  $H$  contains each  $a$ -tuple the same number of times. Consequently, there are  $2^{n-k-1}$  rows in the projection of the  $a$  columns that have even, and  $2^{n-k-1}$  rows that have odd weight.

On the other hand, it is of much larger importance to determine if there exist parity-check matrices with a small number of rows that are free of trapping sets with parameters  $(a;s)$ , for  $1 \leq s \leq b$ , and some small values of  $a$  and  $b$ . For this purpose, we introduce the notion of the *trapping redundancy of a code*.

**Theorem 4.1.** *Let  $C$  be an  $[n;k;d]$  code and  $C^\perp$  its dual. Let  $\mathcal{M}_C(m)$  be the ensemble of all  $m \times n$  matrices with rows chosen independently and at random from the set of  $2^{n-k}$  codewords of  $C^\perp$ , and with replacement. Furthermore, let  $1 \leq a \leq b(d-1) \leq 2n$  be fixed and let  $\Theta(a;b)$  be the number of trapping sets with parameters  $(a;s)$ ;  $1 \leq s \leq b$ ; in a randomly chosen matrix of  $\mathcal{M}_C(m)$ . If*

$$e^{a \frac{n-1}{a-1} \frac{1}{2} \sum_{j=0}^{m-b-1} \binom{m}{j}} > 1; \quad (30)$$

*then  $P\{\Theta(a;b) = 0\} > 0$ . Consequently, if  $m$  satisfies (30), then there exists a parity-check matrix of  $C$  with no more than  $m + n - k - d + 1$  rows and  $\Theta(a;b) = 0$ . The smallest  $m$  for which such a matrix exists is called the  $(a;b)$  trapping redundancy of  $C$ .*

*Proof.* The proof of the claimed result is based on Lovász Local Lemma [46], stated below.

**Lemma 4.1.** [46] *Let  $E_1; E_2; \dots; E_N$  be a set of events in an arbitrary probability space. Suppose that each event  $E_i$  is independent of all other events  $E_j$ , except for at most  $\tau$  of them, and that  $P\{E_i\} \geq p$  for all  $1 \leq i \leq N$ . If*

$$e p (\tau + 1) > 1; \quad (31)$$

*then  $P\{\bigcap_{i=1}^N \overline{E_i}\} > 0$ .*

Let  $E_i$  be the event that the projection of the  $i$ -th collection of  $a$  columns from a randomly chosen matrix in  $\mathcal{M}_C(m)$  contains fewer than  $b$  odd rows. Then

$$P\{E_i\} = \frac{1}{2} \sum_{j=0}^{m-b-1} \binom{m}{j} : \quad (32)$$

Equation (32) follows from the fact that the codewords of the dual code form an orthogonal array of strength  $d - 1$ , and that consequently, even and odd weight rows in the projection are equally likely. This is true independent on the choice of  $a$ , provided that  $1 \leq a \leq b(d - 1) = 2c$ . The restriction on the number of columns  $a$  to lie in the range  $1 \leq a \leq b(d - 1) = 2c$  is imposed in order to ensure that any two events  $E_i$  and  $E_j$  are independent as long as they do not share one or more columns index, since for a linear code with minimum distance  $d$ . In the above setting, let  $\Pr(\bigcap \overline{E_i})$  denote the probability that the randomly chosen matrix is free of trapping sets with parameters  $(a; s)$ , where  $1 \leq s \leq b - 1$ . In order to complete the proof, it suffices to observe that the dependence number of the events  $E_i$  is upper bounded as

$$\tau + 1 \leq a \leq \frac{n - 1}{a - 1};$$

since any subset of  $a$  columns depends on any other subset that shares at least one column with it. Additional  $n - k - d + 1$  rows may be required to make the randomly chosen matrix have rank  $n - k$ .  $\square$

Although Theorem 4.1 ensures the existence of at least one matrix in  $\mathcal{M}_C(m)$  that is free of trapping sets with certain parameters, the actual probability of finding such a matrix may be very small. It is therefore of interest to identify values of the parameter  $m$  for which the probability of obtaining a matrix of the desired form in the ensemble is very close to one.

**Theorem 4.2.** *For a linear code  $C$ , let  $\Theta(a; b)$  be the number of trapping sets with parameters  $(a; s)$ ,  $1 \leq s \leq b - m$ ,  $1 \leq a \leq b(d - 1) = 2c$ , in an  $m \times n$  array from the  $\mathcal{M}_C(m)$  ensemble. Let  $E_i$ ,  $1 \leq i \leq N$  denote the event that the  $i$ -th collection of  $a$  columns contains at least  $b$  rows of odd weight. If*

$$\frac{1}{2} \sum_{j=0}^{m-b-1} \binom{m}{j} \left( \frac{\epsilon}{a} \right)^j \leq 1 - \left( \frac{\epsilon}{a} \right)^{\Theta(a)}; \quad (33)$$

where

$$\Theta(a) = \sum_{l=1}^{a-1} \binom{a}{l} \binom{n-a}{l} = \binom{n}{a} \binom{n-a}{a} \leq 1;$$

then  $\Pr(\Theta(a; b) = 0) > 1 - \epsilon$ .

Consequently, if  $m$  satisfies (33), then there exists a parity-check matrix of  $C$  with no more than  $m + n - k - d + 1$  rows and  $\Theta(a; b) = 0$ .

*Proof.* The result in Equation (33) is obtained by invoking the high-probability variation of Lovász Local Lemma, stated below.

**Lemma 4.2.** [46] Let  $E_1; E_2; \dots; E_N$  be a set of events in an arbitrary probability space, and let  $0 < \varepsilon < 1$ . Suppose that each event  $E_i$  is independent from all other events  $E_j$ , except for at most  $\tau$  of them. If

$$P(E_i) \geq \frac{\varepsilon}{N} \quad 1 \leq i \leq N;$$

then  $P(\bigcap_{i=1}^N \overline{E_i}) > 1 - \varepsilon$ .

To prove the theorem, replace the expression for  $P(E_i)$  in the above result by Equation (32). The number of events  $E_i$ ,  $N$ , can easily be seen to be  $\binom{n}{a}$ , and  $\tau$ , the number of events dependent on a fixed event  $E_i$  equals  $\tau = \sum_{l=1}^a \binom{a-l}{a-l} \binom{n-l}{a-l}$ . The claimed result follows by invoking Vandermonde's convolution formula [47] which states that

$$\sum_{t+l=u} \binom{r}{t} \binom{s}{l} = \binom{r+s}{u};$$

for some integers  $t$  and  $u$ . □

Although a closed form for Equation (33) in terms of  $m$  does not exist, it can be accurately approximated in terms of the following results from [47, p. 240].

Let

$$A_m = \sum_{i=0}^m \binom{m}{i} \lambda^i;$$

where  $0 < \lambda < 1$ . The asymptotic formula for  $A_m$  depends on the particular value of  $\lambda$ :

(a)  $\lambda = 1/2$ :

$$A_m \sim 2^{m-1}$$

(b)  $\lambda > 1/2$ :

$$A_m \sim 2^m;$$

independently on the precise value of  $\lambda$ .

(c)  $\lambda < 1/2$ :

$$A_m \sim \frac{m}{\ln m} \frac{1}{1 - \lambda}:$$

Consequently, by replacing  $\lambda$  with  $(b-1)/m$  one obtains the following results.

(a) For  $b = m=2 + 1, \lambda = 1=2$  so that Equation (33) can be used to bound  $m$  as

$$2^{m-1} \geq \frac{\epsilon}{a} \left(1 - \frac{\epsilon}{a}\right)^{\binom{n}{a} - \binom{n-a}{a} - 1}; \text{ i.e.} \\ m \geq \frac{n}{a} - \frac{n-a}{a} + 1 + \log_2 \left( \frac{\epsilon}{a} \left(1 - \frac{\epsilon}{a}\right)^{\binom{n}{a} - \binom{n-a}{a} - 1} \right); \quad (34)$$

where the logarithm is taken base two.

(b) For  $b > m=2 + 1, \lambda > 1=2$  holds, and Equation (33) can be used to bound  $m$  as

$$2^m \geq \frac{\epsilon}{a} \left(1 - \frac{\epsilon}{a}\right)^{\binom{n}{a} - \binom{n-a}{a} - 1}; \text{ i.e.} \\ m \geq \frac{n}{a} - \frac{n-a}{a} + 1 + \log_2 \left( \frac{\epsilon}{a} \left(1 - \frac{\epsilon}{a}\right)^{\binom{n}{a} - \binom{n-a}{a} - 1} \right); \quad (35)$$

where the logarithm is taken base two.

(c) For  $b < m=2 + 1$ , with  $b = \lfloor \lambda m \rfloor + 1, \lambda < 1=2$  so that Equation (33) reduces to

$$\frac{1}{2} \leq \frac{m}{\lfloor \lambda m \rfloor + 1} \frac{1}{1 - \frac{\lambda}{1-\lambda}} \left( \frac{\epsilon}{a} \left(1 - \frac{\epsilon}{a}\right)^{\binom{n}{a} - \binom{n-a}{a} - 1} \right); \quad (36)$$

The question remains how tight the bounds on the trapping redundancy and its high probability equivalent are. Testing these bounds for long codes is a computationally intractable problem. Therefore, we compare the above bounds to *analytically obtained exact trapping redundancy values* for codes based on projective geometries, as described in Appendix B. Furthermore, we evaluate the bounds for the Margulis code and show that in this case, very few redundant rows are actually required to eliminate all  $(12;4)$  and  $(14;4)$  trapping sets.

**Remark – A word of caution:** The matrices from the ensemble  $\mathcal{M}(m)$  have, in general, highly non-uniform row and column weights. The variable and check node degrees of their corresponding Tanner graph may also be very large, leading to the emergence of short cycles. Consequently, the results above are to be used as performance benchmarks, an practically applied only for very small redundancy values.

## 5 Conclusions and Future Work

We presented two methods for reducing the height of the error floor in LDPC codes: one, based on changing the message update rules in BP decoding, and another, based on adding redundant parity-check nodes to the Tanner graph of the underlying codes. Although our study was focused on the Margulis  $[2640;1320]$  code, all results presented in this work apply to other classes of codes as well.

These two techniques are by no means the only methods that can be used to reduce the error floor of LDPC codes. Other approaches, such as combining BP decoders and *permutation decoding*, or statistically combining outputs of several different BP decoders ran in parallels are currently under investigation.

## A Proofs of Section 3

This section contains the proofs of the four lemmas in Section 3 pertaining to the noise threshold  $s^2$  of several form of averaged decoding. The proofs proceed in two steps. The first step consists in proving that elements of the sequence  $\hat{t}_l(s)$  are strictly increasing. The second step consists in showing that the sequence does not have a finite limit. The second step is a straightforward consequence of the fact that the sequence  $\hat{t}_l(s)$  described in terms of the functions  $f(s; t)$  and  $\phi(x)$  cannot have finite fixed points, provided that its terms are strictly increasing. Consequently, we only provide the proofs for the first step.

### A.1 Proof of Lemma 3.1

Let us show by induction that the sequence  $\hat{t}_l(s)$  is strictly increasing for  $l \leq l_{av}$ . The basis for induction is given by

$$\begin{aligned}\hat{t}_0(s) &= t_0(s) = 0 \\ \hat{t}_1(s) &= f(s; \hat{t}_0(s)) = f(s; t_0(s)) = t_1(s) > 0 \\ \hat{t}_2(s) &= \frac{1}{2} [\hat{t}_1(s) + f(s; \hat{t}_1(s))] = \frac{1}{2} [\hat{t}_1(s) + f(s; t_1(s))] \\ &> \frac{1}{2} [\hat{t}_1(s) + t_1(s)] = \frac{1}{2} [\hat{t}_1(s) + \hat{t}_1(s)] = \hat{t}_1(s)\end{aligned}\tag{37}$$

Assume that  $\hat{t}_l(s)$  is increasing up to  $l = L < l_{av}$ . Then

$$\begin{aligned}\hat{t}_{L+1}(s) - \hat{t}_L(s) &= \frac{1}{L+1} (f(s; \hat{t}_L(s)) + \hat{t}_L(s) + \hat{t}_{L-1}(s) + \hat{t}_{L-2}(s) + \dots + \hat{t}_1(s)) \\ &\quad - \frac{1}{L} (f(s; \hat{t}_{L-1}(s)) + \hat{t}_{L-1}(s) + \hat{t}_{L-2}(s) + \dots + \hat{t}_1(s)) \\ &= \frac{1}{L+1} (f(s; \hat{t}_L(s)) - f(s; \hat{t}_{L-1}(s))) \\ &\quad + \frac{1}{L+1} \hat{t}_L(s) - \frac{1}{L} (f(s; \hat{t}_{L-1}(s)) + \hat{t}_{L-1}(s) + \hat{t}_{L-2}(s) + \dots + \hat{t}_1(s)) \\ &> 0 \quad \text{for } L < l_{av}:\end{aligned}\tag{38}$$

Here, we used the decomposition

$$\frac{1}{L} = \frac{(L+1)}{(L+1)} \frac{1}{L} = \frac{1}{L+1} + \frac{1}{L} \frac{1}{(L+1)};\tag{39}$$



The inequality in Equation (38) holds since the second sum in the expression equals zero by definition (25), and  $\hat{t}_L(s) > \hat{t}_{L-1}(s)$  by induction hypothesis, so that  $f(s; \hat{t}_L(s)) > f(s; \hat{t}_{L-1}(s))$ , since  $f(s; t)$  is strictly increasing in  $t$ .

We show next that the sequence  $\hat{t}_l(s)$  is also strictly increasing for all  $l > l_{av}$ . Let us assume this property holds up to some iteration  $l = L$ , where  $L > l_{av}$ . The following argument shows that the monotonicity property also has to hold for  $l > L$ :

$$\begin{aligned} \hat{t}_{L+1}(s) - \hat{t}_L(s) &= \frac{1}{l_{av}} (f(s; \hat{t}_L(s)) + \hat{t}_L(s) + \hat{t}_{L-1}(s) + \dots + \hat{t}_{L-l_{av}+2}(s)) \\ &\quad - \frac{1}{l_{av}} (f(s; \hat{t}_{L-1}(s)) + \hat{t}_{L-1}(s) + \hat{t}_{L-2}(s) + \dots + \hat{t}_{L-l_{av}+1}(s)) \\ &= \frac{1}{l_{av}} (f(s; \hat{t}_L(s)) - f(s; \hat{t}_{L-1}(s)) + \hat{t}_L(s) - \hat{t}_{L-l_{av}+1}(s)) > 0; \end{aligned} \quad (40)$$

where the inequality is true since  $\hat{t}_l(s)$  is strictly increasing for all  $l \leq L$ . This completes the proof.

## A.2 Proof of Lemma 3.2

To prove the lemma, we show that  $\check{t}_l(s) > \check{t}_{l-1}(s) \forall l$ . The starting point is to prove that  $\check{t}_l(s) > \check{t}_{l-1}(s)$  for  $0 \leq l \leq l_{av}$ . The basis assumptions for induction are:

$$\begin{aligned} \check{t}_0(s) &= t_0(s) = 0; \\ \check{t}_1(s) &= f(s; \check{t}_0(s)) = f(s; t_0(s)) = t_1(s) > 0; \quad \check{t}_2(s) = \frac{f(s; \check{t}_1(s)) - \check{t}_1(s)}{f(s; \check{t}_1(s)) - \check{t}_1(s)} = \frac{f(s; \check{t}_1(s)) - \check{t}_1(s)}{f(s; \check{t}_1(s)) - \check{t}_1(s)} = \check{t}_1(s) \end{aligned}$$

To show that  $\check{t}_3(s) > \check{t}_2(s)$ , consider

$$\begin{aligned} \frac{\check{t}_3(s)}{\check{t}_2(s)} &= \frac{\frac{f(s; \check{t}_2(s)) - \check{t}_2(s)}{f(s; \check{t}_1(s)) - \check{t}_1(s)}}{\frac{f(s; \check{t}_1(s)) - \check{t}_1(s)}{f(s; \check{t}_1(s)) - \check{t}_1(s)}} = \frac{f(s; \check{t}_2(s))^{1=3} \check{t}_2(s)^{1=3} \check{t}_1(s)^{1=3}}{f(s; \check{t}_1(s))^{1=2} \check{t}_1(s)^{1=2}} \\ &= \frac{\check{t}_1(s)^{1=3}}{\check{t}_1(s)^{1=3}} \frac{\check{t}_2(s)^{1=3}}{(f(s; \check{t}_1(s)) - \check{t}_1(s))^{1=6}} \frac{f(s; \check{t}_2(s))^{1=3}}{f(s; \check{t}_1(s))^{1=3}}; \end{aligned} \quad (41)$$

Clearly, the first and second term in the above expression equal to one, while the third term is strictly greater than one since  $f(s; t)$  is a strictly increasing function in  $t$  and  $\check{t}_2(s) > \check{t}_1(s)$ .

Let us show next that  $\check{t}_{L+1}(s) > \check{t}_L(s)$  for all  $L > l_{av}$ . Consider the ratio of  $\check{t}_{L+1}(s) / \check{t}_L(s)$ , for  $L > l_{av}$ , and rewrite it according

to (26) as

$$\begin{aligned}
\frac{\check{t}_{L+1}(s)}{\check{t}_L(s)} &= \frac{\prod_{i=1}^L \check{t}_i(s)}{\prod_{i=1}^L f(s; \check{t}_{L-1}(s))} \\
&= \frac{f(s; \check{t}_L(s))^{1=L}}{f(s; \check{t}_{L-1}(s))^{1=L} f(s; \check{t}_{L-1}(s))^{1=(L+1)L}} \frac{\prod_{i=1}^L \check{t}_i(s)^{1=(L+1)}}{\prod_{i=1}^L \check{t}_i(s)^{1=(L+1)} \prod_{i=1}^L \check{t}_i(s)^{1=(L+1)L}} \\
&= \frac{f(s; \check{t}_L(s))^{1=(L+1)}}{f(s; \check{t}_{L-1}(s))^{1=(L+1)} \prod_{i=1}^L \check{t}_i(s)^{1=(L+1)} f(s; \check{t}_{L-1}(s))^{1=(L+1)L} \prod_{i=1}^L \check{t}_i(s)^{1=(L+1)L}} \\
&= \frac{f(s; \check{t}_L(s))^{1=(L+1)}}{f(s; \check{t}_{L-1}(s))^{1=(L+1)}} \frac{\check{t}_L(s)^{1=(L+1)}}{f(s; \check{t}_{L-1}(s))^L \prod_{i=1}^L \check{t}_i(s)^{1=(L+1)}} \\
&= \frac{f(s; \check{t}_L(s))^{1=(L+1)}}{f(s; \check{t}_{L-1}(s))^{1=(L+1)}} \frac{\check{t}_L(s)^{1=L}}{\check{t}_L(s)^{1=(L+1)L}} > 1 \quad 8L < l_{av} :
\end{aligned} \tag{42}$$

Assume next that the sequence  $\check{t}_l(s)$  is strictly for all values of  $l < L$ . Then

$$\begin{aligned}
\frac{\check{t}_{L+1}(s)}{\check{t}_L(s)} &= \frac{\prod_{i=L}^{l_{av}} f(s; \check{t}_{L+1}(s)) \prod_{i=L}^{l_{av}+2} \check{t}_i(s)}{\prod_{i=L}^{l_{av}} f(s; \check{t}_{L-1}(s)) \prod_{i=L}^{l_{av}+1} \check{t}_i(s)} \\
&= \frac{s \frac{f(s; \check{t}_L(s))}{f(s; \check{t}_{L-1}(s))}}{s \frac{\check{t}_L(s) \prod_{i=L}^{l_{av}+2} \check{t}_i(s)}{\check{t}_L(s)^{l_{av}+1} \prod_{i=L}^{l_{av}+2} \check{t}_i(s)}} \\
&= \frac{s \frac{f(s; \check{t}_L(s))}{f(s; \check{t}_{L-1}(s))}}{s \frac{\check{t}_L(s)}{\check{t}_L(s)^{l_{av}+1}}} > 1;
\end{aligned} \tag{43}$$

which completes the proof.

### A.3 Proof of Lemma 3.3

We start by observing that  $\tilde{t}_1(s) > \tilde{t}_0(s) = 0$  and  $\tilde{t}_2(s) > \tilde{t}_1(s)$ . Assume that the induction hypothesis is that  $\tilde{t}_l(s) > \tilde{t}_{l-1}(s)$  for all  $l < L$ .

Consider Equation (28), and write

$$a(l) = \frac{e^{\tilde{t}_l(s)}}{1 + e^{\tilde{t}_l(s)}} \tag{44}$$

$$b(l) = \frac{e^{f(s; \tilde{t}_l(s))}}{1 + e^{f(s; \tilde{t}_l(s))}} : \tag{45}$$

Clearly,  $0 < a(l) < 1$  and  $0 < b(l) < 1$  for all  $l > 0$ .

The function  $e^x = (1 + e^x)$  is strictly increasing with  $x$ , and by induction hypothesis,  $\tilde{t}_l(s)$  is strictly increasing with  $l$ , so that  $\tilde{t}_l(s) > \tilde{t}_{l-1}(s)$  for  $l < L$ . Consequently,  $f(s; \tilde{t}_l(s)) > f(s; \tilde{t}_{l-1}(s))$  holds. This implies that  $a(l) > a(l-1)$  and  $b(l) > b(l-1)$  for  $l < L$ .

Now, Equation (28) can be rewritten as

$$\tilde{t}_l(s) = \log \frac{1 - \prod_{k=1}^l \frac{a(k-1) - b(k-1)}{a(k) - b(k)}}{1 - \prod_{k=1}^l \frac{a(k-1) - b(k-1)}{a(k) - b(k)}}; \quad (46)$$

To show that  $\tilde{t}_{L+1}(s) > \tilde{t}_L(s)$ , we take the difference of these two terms and use Equation (46) to obtain

$$\begin{aligned} \tilde{t}_{L+1}(s) - \tilde{t}_L(s) &= \log \frac{1 - \prod_{k=1}^L \frac{a(k) - b(k)}{a(k) - b(k)}}{1 - \prod_{k=1}^L \frac{a(k-1) - b(k-1)}{a(k) - b(k)}} - \log \frac{1 - \prod_{k=1}^{L-1} \frac{a(k-1) - b(k-1)}{a(k) - b(k)}}{1 - \prod_{k=1}^{L-1} \frac{a(k-1) - b(k-1)}{a(k) - b(k)}} \\ &= \log \frac{1 - \prod_{k=1}^L \frac{a(k) - b(k)}{a(k) - b(k)}}{1 - \prod_{k=1}^L \frac{a(k-1) - b(k-1)}{a(k) - b(k)}} \\ &= \log \frac{1 - \prod_{k=1}^L \frac{a(k)}{a(k-1)} \frac{b(k)}{b(k-1)}}{1 - \prod_{k=1}^L \frac{a(k-1) - b(k-1)}{a(k) - b(k)}} \\ &= \log \frac{1 - \prod_{k=1}^L \frac{a(k)}{a(k-1)} \frac{b(k)}{b(k-1)}}{1 - \prod_{k=1}^L \frac{a(k-1) - b(k-1)}{a(k) - b(k)}} + \log \frac{1 - \prod_{k=1}^{L-1} \frac{a(k-1) - b(k-1)}{a(k) - b(k)}}{1 - \prod_{k=1}^{L-1} \frac{a(k-1) - b(k-1)}{a(k) - b(k)}} \\ &> \log \frac{1 - \prod_{k=1}^L \frac{a(k-1) - b(k-1)}{a(k) - b(k)}}{1 - \prod_{k=1}^L \frac{a(k-1) - b(k-1)}{a(k) - b(k)}}; \end{aligned} \quad (47)$$

The last inequality holds since  $a(k) > a(k-1)$  and  $b(k) > b(k-1)$ .

Since  $0 < a(k-1) < a(k) < 1$  and  $0 < b(k-1) < b(k) < 1$ , one has

$$0 < a(k-1) - b(k-1) < a(k) - b(k) < 1;$$

and consequently

$$0 < \frac{1 - \prod_{k=1}^L \frac{a(k-1) - b(k-1)}{a(k) - b(k)}}{1 - \prod_{k=1}^L \frac{a(k-1) - b(k-1)}{a(k) - b(k)}} < 1;$$

From the above inequality it directly follows that

$$1 > \frac{1 - \prod_{k=1}^L \frac{a(k-1) - b(k-1)}{a(k) - b(k)}}{1 - \prod_{k=1}^L \frac{a(k-1) - b(k-1)}{a(k) - b(k)}} > 1 - \prod_{k=1}^L \frac{a(k-1) - b(k-1)}{a(k) - b(k)} > 0;$$

so that

$$\tilde{t}_l(s) - \tilde{t}_L(s) > \log \frac{1 - \prod_{k=1}^L \frac{a(k-1) - b(k-1)}{a(k) - b(k)}}{1 - \prod_{k=1}^L \frac{a(k-1) - b(k-1)}{a(k) - b(k)}} > \log 1 = 0;$$

Therefore,  $\tilde{t}_l(s) > \tilde{t}_L(s)$  for all  $l > 0$ , which completes the proof.

## A.4 Proof of Equation (28)

The induction steps proceed along the same line as outlined in the previous section. For  $t_l^0(s) = \log \frac{p_l^0}{1 - p_l^0}$  one has

$$\begin{aligned}
 t_l^0(s) &= \log \frac{p_l^0}{1 - p_l^0} \\
 &= \log \frac{1}{l_{av}} \frac{e^{f(s; \frac{e^{p_l^0-1}}{e^{p_l^0-1}})}}{1 + e^{f(s; \frac{e^{p_l^0-1}}{e^{p_l^0-1}})}} + \sum_{i=1}^{l_{av}-1} \frac{e^{t_{l-i}^0(s)}}{1 + e^{t_{l-i}^0(s)}} \\
 &= \log \frac{1}{l_{av}} \frac{e^{f(s; \frac{e^{p_l^0-1}}{e^{p_l^0-1}})}}{1 + e^{f(s; \frac{e^{p_l^0-1}}{e^{p_l^0-1}})}} + \sum_{i=1}^{l_{av}-1} \frac{e^{t_{l-i}^0(s)}}{1 + e^{t_{l-i}^0(s)}} : 
 \end{aligned} \tag{48}$$

For simplicity of notation, let

$$a(l) = \frac{e^{t_l^0(s)}}{1 + e^{t_l^0(s)}} \tag{49}$$

$$b(l) = \frac{e^{f(s; \frac{e^{p_l^0-1}}{e^{p_l^0-1}})}}{1 + e^{f(s; \frac{e^{p_l^0-1}}{e^{p_l^0-1}})}} : \tag{50}$$

so that Equation (48) becomes

$$t_l^0(s) = \log \frac{1}{l_{av}} (b(l-1) + \sum_{i=1}^{l_{av}-1} a(l-i)) = \log \frac{1}{l_{av}} (b(l-1) + \sum_{i=1}^{l_{av}-1} a(l-i)) \tag{51}$$

Consider

$$\begin{aligned}
 t_l^0(s) - t_{l-1}^0(s) &= \log \frac{1}{l_{av}} (b(l-1) + \sum_{i=1}^{l_{av}-1} a(l-i)) - \log \frac{1}{l_{av}} (b(l-2) + \sum_{i=1}^{l_{av}-1} a(l-i)) \\
 &= \log \frac{1}{l_{av}} (b(l-1) + \sum_{i=1}^{l_{av}-1} a(l-i)) - \log \frac{1}{l_{av}} (b(l-2) + \sum_{i=1}^{l_{av}-1} a(l-i)) \\
 &= \log \frac{1}{l_{av}} \frac{b(l-1) + \sum_{i=1}^{l_{av}-1} a(l-i)}{b(l-2) + \sum_{i=1}^{l_{av}-1} a(l-i)} + \log \frac{1}{1} \frac{b(l-2) + \sum_{i=1}^{l_{av}-1} a(l-i)}{b(l-1) + \sum_{i=1}^{l_{av}-1} a(l-i)} : 
 \end{aligned} \tag{52}$$

It is tedious, but straightforward to show that the arguments of both logarithms are strictly larger than one. This completes the proof of the claimed result.

## B Trapping sets and Redundancy: Projective Geometry and Margulis Codes

We compare the analytical upper bounds derived in Section 4 with results obtained from a case-study of the class of projective geometry. The purpose of this comparison is twofold: first, it allows one to see how tight the upper bounds on the trapping redundancy are, and secondly, it provides an example of a class of codes that does not have small trapping sets and consequently may not require the use of any specialized averaging techniques. Furthermore, we also find upper

bounds on the number of redundant rows one needs to add to the standard parity-check matrix of the  $[2640;1320]$  Margulis code in order to eliminate all  $(12;4)$  and  $(14;4)$  trapping sets.

## B.1 Trapping sets in Projective Geometry Codes

We start by introducing the relevant terminology.

**Definition B.1.** A finite projective geometry  $PG(m; q)$  of dimension  $m$  and over a finite field  $GF(q)$ , for some prime power  $q$ , is a collection of points and subsets of the point set called lines, for which the following axioms hold true [48]:

Two distinct points determine a unique line;

Every line consists of more than two points;

For every pair of distinct lines  $L_1$  and  $L_2$ , intersecting at some point  $r$ , there exist two pairs of points  $(p_1; q_1) \in L_1$  and  $(p_2; q_2) \in L_2$  that differ from  $r$ , such that the lines determined by  $(p_1; p_2)$  and  $(q_1; q_2)$  intersect as well.

For each point and for each line, there exist at least two lines and two points that are not incident to them, respectively.

The points of a projective geometry  $PG(m; q)$  can be represented by non-zero  $(m+1)$ -tuples  $(a_0; a_1; a_2; \dots; a_m)$  such that  $a_i \in GF(q)$ . Points of the form  $(a_0; a_1; a_2; \dots; a_m)$  and  $(\delta a_0; \delta a_1; \delta a_2; \dots; \delta a_m)$ ,  $\delta \in GF(q) \setminus \{0\}$ , are considered to be equivalent. A line through two distinct points  $(a_0; a_1; a_2; \dots; a_m)$  and  $(b_0; b_1; b_2; \dots; b_m)$  consists of all points that can be expressed as  $(\alpha a_0 + \beta b_0; \dots; \alpha a_m + \beta b_m)$ , where  $\alpha; \beta \in GF(q)$  and are not simultaneously zero. Consequently, a projective geometry  $PG(m; q)$  has  $(q^{m+1} - 1)/(q - 1) = (q^m + \dots + q + 1)$  points, and each line in the geometry contains  $q + 1$  points. The number of lines in a projective geometry is given by

$$(q^m + \dots + q + 1)(q^{m-1} + \dots + q + 1) \dots (q + 1) = (q + 1)^m \quad (53)$$

A type-I projective geometry code is defined in terms of a parity-check matrix representing the *line-point* incidence matrix of a projective geometry  $PG(m; q)$  [49]. We consider projective plane codes, for which  $m = 2$ , and codes based on projective geometries with  $m = 3$  only.

**Definition B.2.** An  $s$ -arc in  $PG(2; q)$  is a collection of  $s$  points such that no three of them are collinear. The lines incident to an  $s$ -arc  $\mathcal{K}$  are either unisecants (they intersect the arc in exactly one point) or bisecants (they intersect the arc in exactly two points). Similarly, an  $s$ -cap in  $PG(3; q)$  is a set of  $s$  points, no three of which are collinear.

The following results are taken from [50, pp. 176-200] and [51, pp. 33-52].

**Lemma B.1.** *Let  $\tau_1$  and  $\tau_2$  denote the number of unisecants and bisecants of an  $s$ -arc  $\mathcal{K}$  in  $PG(2; q)$ . Then*

$$\tau_1 = s(q + 2 - s); \text{ and } \tau_2 = \frac{1}{2}s(s - 1); \quad (54)$$

*Similarly, for an  $s$ -cap  $\mathcal{K}$  in  $PG(3; q)$  it holds that:*

$$\tau_1 = q^2 + q + 2 - s; \quad (55)$$

*where  $\tau_1$  denotes the number of unisecants of  $\mathcal{K}$ .*

**Lemma B.2.** *The largest arc in  $PG(2; q)$  contains at most  $q + 2$  points, for  $q$  even, and  $q + 1$  points, for  $q$  odd. Arcs with  $s = q + 1$  and  $s = q + 2$  are called ovals and hyperovals, respectively. The size of any  $s$ -cap in  $PG(3; q)$  satisfies  $s \leq q^2 + 1$ . For  $q > 1$ , an  $q^2 + 1$ -cap is called an ovaloid.*

The results of Lemma B.1 and B.2 can be used to establish the following results regarding trapping sets in the graph of type-I projective geometry codes.

**Corollary B.1.** *All elementary trapping sets of a  $PG(2; q)$ , type-I projective geometry code have parameters  $(s; s(q + 2 - s))$ . Consequently, the number of degree-one check nodes of such trapping sets for  $q$  odd is necessarily larger than or equal to the number of variables in the trapping set. For even values of  $q$ , an exception to the aforementioned finding is a hyperoval, which represents a stopping set. The trapping sets with the smallest and largest ratio  $b/a$  have parameters  $(q + 1; q + 1)$  ( $q$  odd) and  $(3; 3(q - 1))$ , respectively. A trapping set with  $a = (q + 3)/2$  (if such a set exists) has the smallest ratio of satisfied  $\tau_2$  and unsatisfied  $\tau_1$  checks, which in this case equals to one.*

**Corollary B.2.** *All elementary trapping sets of a  $PG(3; q)$ , type-I projective geometry code have parameters  $(s; q^2 + q + 2 - s)$ . The trapping sets with the smallest and largest ratio  $b/a$  have parameters  $(q^2 + 1; q + 1)$  and  $(3; q^2 + q - 1)$ .*

**Remark:** From the 21 trapping sets identified in the test-codes of [5], only two were of the form  $(a; b)$  with  $a < b$ , namely  $(3; 9)$  and  $(4; 10)$ . The first trapping set contributed to 27, while the other contributed to 13 failures. In addition, the largest trapping set in the list contains 16 variables. For  $s = 16$ ,  $q = 2^5 = 32$ , a hypothetical trapping set in a type-I  $PG(2; q)$  code would have 288 checks of degree one.

A complete classification of trapping sets in projective geometry codes is probably an impossible task. This is due to the fact that very little is known about the number and existence of arcs and caps of different sizes in projective spaces.

One aspect of this problem that is better understood is the existence and enumeration of *complete arcs* (and *caps*) - i.e. arcs and caps not contained in any larger arc or cap. Results pertaining to the enumeration of these configurations will be presented elsewhere.

Some examples of projective geometry codes and their smallest trapping sets are given in Table 7. In this table, *complete H* refers to the size of the parity-check matrix in terms of a complete set of lines and points of the geometry. Furthermore, in Tables 8 and 9, let *minimal H* denotes a matrix with  $n - k - n$  (i.e. a matrix for which some projective lines were removed in order to ensure that the matrix has rank  $n - k$  and only  $n - k$  rows). The size of the parity-check matrix derived using Lovász Local Lemma and its high-probability variation in Theorems 4.1 and 4.2 are denoted by *LLL H (standard)* and *LLL H (high probability)*, respectively.

Code	dimensions	smallest trapping sets
$PG(2;16)$	273 273	$(3;42), :: (s_2; s_2(16 + 2 - s_2)), :: (8;80), (9;81), (10;80), :: (17;17)$
$PG(2;32)$	1057 1057	$(3;93), :: (s_2; s_2(32 + 2 - s_2)), :: (16;288), (17;289), (18;288), :: (33;33)$

Table 7: Parameters of the smallest trapping sets for three selected  $PG(m;q)$  codes, where  $3 \leq s_2 \leq q + 2$  for  $m = 2$ , and  $s_3 \leq (q^2 + q + 2)/5$ ,  $s_3 \leq (q^3 + q^2 + q + 1)/3$  for  $m = 3$ .

The values for the minimum distance and the rank of the parity-check matrix,  $n - k$ , are taken from [49].

Code	Trapping set size		complete $H$	minimal $H$	LLL $H$ (standard)	LLL $H$ (high probability)	
	$a$	$b$				$\epsilon = 0.01$	$\epsilon = 10^{-20}$
$PG(2;16)$	17	17	273 273	82 273	228 273	230 273	302 273
$PG(2;32)$	33	33	1057 1057	244 1057	574 1057	579 1057	647 1057

Table 8: Necessary size of the parity-check matrix for selected PG codes to be free of  $(a;s)$  trapping sets with  $1 \leq s < b$ . The size of  $H$  from the PG code construction (complete  $H$ ), the effective codimension  $n - k$  (minimal  $H$ ), and the minimum size of the parity-check matrix derived using Theorems 4.1 and 4.2 (LLL  $H$  (standard) and (high probability)) are shown.

## B.2 Bounds for the $[2640;1320]$ Margulis Code

Results similar to those derived for projective geometry codes are shown for the  $[2640;1320]$  Margulis code in Table 9.

We used the estimate  $d \geq 40$  [52] for this code.

It can be seen from Table 9 that there exists a redundant parity-check matrix with at most 1426 rows that does not contain any trapping sets of size  $(14;s)$  with  $1 \leq s < 5$ .

$a$	$b$	minimal $H$		LLL $H$ (standard)		LLL $H$ (high probability)			
						$\epsilon = 0.01$		$\epsilon = 10^{-20}$	
6	5	1320	2640	1356	2640	1320	2640	1431	2640
8	5	1320	2640	1375	2640	1386	2640	1448	2640
12	5	1320	2640	1410	2640	1419	2640	1481	2640
14	5	1320	2640	1426	2640	1435	2640	1497	2640
22	5	1320	2640	1487	2640	1494	2640	1556	2640

Table 9: Necessary size of the parity-check matrix of the  $[2640;1320]$  Margulis code to be free of trapping sets of size  $(a;s)$ ,  $1 \leq s < b$ . The columns show the effective codimension of the code (minimal  $H$ ), and lower bounds on the size of  $H$  derived from Theorems 4.1 and 4.2 (LLL  $H$  (standard) and (high probability)).

## References

- [1] J. Rosenthal and P. Vontobel, “Constructions of regular and irregular LDPC codes using Ramanujan graphs and ideas from Margulis,” in *Proc. Int. Symp. Inform. Theory (ISIT’01)*, (Washington D.C.), p. 4, June 24–29 2001.
- [2] O. Milenkovic, D. Leyba, and N. Kashyap, “Shortened array codes of large girth,” *IEEE Trans. on Inform. Theory*, vol. 5, pp. 3707–3722, Aug. 2006.
- [3] S. Laendner and O. Milenkovic, “Codes based on latin squares: Stopping set, trapping set, and cycle-length distribution analysis,” *IEEE Trans. on Comm.*, February 2007.
- [4] D. MacKay and M. Postol, “Weaknesses of Margulis and Ramanujan-Margulis low-density parity-check codes,” *Electronic Notes in Theoretical Computer Science*, vol. 74, 2003.
- [5] T. Richardson, “Error-floors of LDPC codes,” in *Proceedings of the 41st Annual Allerton Conference on Communication, Control and Computing*, pp. 1426–1435, Sept. 2003.
- [6] C. Di, D. Proletti, I. Telatar, T. Richardson, and R. Urbanke, “Finite length analysis of low-density parity-check codes,” *IEEE Trans. on Inform. Theory*, vol. 48, pp. 1570–1579, June 2002.
- [7] P. Vontobel and R. Koetter, “Graph-cover decoding and finite-length analysis of message-passing iterative decoding of LDPC codes,” *submitted to IEEE Trans. on Inform. Theory*, Dec. 2005.
- [8] J. Feldman, *Decoding Error-Correcting Codes via Linear Programming*. PhD thesis, Massachusetts Institute of Technology, Cambridge, MA, 2003.
- [9] R. Smarandache and P. Vontobel, “Pseudo-codeword analysis of tanner graphs from projective and euclidean planes,” *submitted to IEEE Trans. Inform. Theory*, available online under <http://www.arxiv.org/abs/cs.IT/0602089>, Feb. 2006.
- [10] R. Smarandache and M. Waurer, “Bounds on the pseudo-weight of minimal pseudo-codewords of projective geometry codes,” *Contemporary Mathematics*, available online.
- [11] M. Stepanov, V. Chernyak, M. Chertkov, and B. Vasic, “Diagnosis of weaknesses in modern error correction codes: a physics approach,” pp. 1–9, June 2005.
- [12] M. Stepanov and M. Chertkov, “Improving convergence of belief propagation decoding,” in *Proceedings of the 44th Annual Allerton Conference on Communication, Control and Computing*, (Monticelli, IL), Sept. 2006.
- [13] C. Cole, S. Wilson, E. Hall, and T. Giallorenzi, “A general method for finding low error rates of ldpc codes,” pp. 1–30, 2006.



- [14] A. Montanari, "The asymptotic error floor of LDPC ensembles under BP decoding," in *Proceedings of the 44th Annual Allerton Conference on Communication, Control and Computing*, Sept. 2006.
- [15] M. Pretti, "A message-passing algorithm with damping," *J. Stat. Mech.*, Nov. 2005.
- [16] R. Clemen and R. Winkler, "Combining probability distributions from experts in risk analysis," *Risk Analysis*, vol. 19, pp. 187–204, 1999.
- [17] G. Hardy, *Divergent series*. AMS Chelsea Publishing, 1991.
- [18] S. Laendner and O. Milenkovic, "Algorithmic and combinatorial analysis of trapping sets in structured LDPC codes," in *Proceedings of the International Conference on Wireless Networks, Communications, and Mobile Computing (WirelessComm2005)*, (Maui, Hawaii), June 2005.
- [19] R. Koetter, "Iterative coding techniques, pseudocodewords, and their relationship," in *Workshop on Applications of Statistical Physics to Coding Theory*, (Santa Fe, New Mexico), January 2005.
- [20] M. Schwartz and A. Vardy, "On the stopping distance and stopping redundancy of codes," *submitted to IEEE Trans. on Inform. Theory*, March 2005.
- [21] D. MacKay, *Information Theory, Inference, and Learning Algorithms*. Cambridge University Press, 2003.
- [22] J. Thorpe, "Low-complexity approximations to belief propagation for ldpc codes," pp. 980–984, July 2003.
- [23] Z. Zhang, L. Dolecek, B. Nikolic, V. Anantharam, and M. Wainwright, "Investigation of error floors of structured low-density parity-check codes by hardware emulation," *Proceedings of the 49th annual IEEE Global Telecommunications Conference (GlobeCom 2006)*, Nov. 2006.
- [24] M. Tanner, "A recursive approach to low complexity codes," *IEEE Trans. on Inform. Theory*, vol. 27, pp. 533–547, Sept. 1981.
- [25] I. Kozintsev, "Website, <http://www.kozintsev.net/soft.html>,"
- [26] D. J. C. MacKay and R. M. Neal, "Near Shannon limit performance of low-density parity-check codes," *Electronic Letters*, vol. 32, pp. 1645–1646, 1996.
- [27] O. Milenkovic, E. Soljanin, and P. Whiting, "Asymptotic spectra of trapping sets in regular and irregular ldpc code ensembles," *to appear in IEEE Trans. Inform. Theory*, Jan. 2007.
- [28] M. R. Yazdani, S. Hemati, and A. H. Banihashemi, "Improving belief propagation on graphs with cycles," *IEEE Comm. Letters*, vol. 8, pp. 57–59, Jan 2004.
- [29] J. Chen and M. Fossorier, "Density evolution for two improved bp-based decoding algorithms of ldpc codes," *IEEE Communications Letters*, vol. 6, pp. 208–210, May 2002.
- [30] J. Jiang and K. Narayanan, "Iterative soft decoding of reed-solomon codes," *IEEE Comm. Letters*, vol. 8, pp. 244–246, April 2004.
- [31] J. Jiang and K. Narayanan, "Iterative soft-input soft-output decoding of reed-solomon codes by adapting the parity-check matrix," *IEEE Trans. on Inform. Theory*, vol. 52, pp. 3746–3756, August 2006.
- [32] M. El-Khamy and R. McEliece, "Iterative algebraic soft-decision list decoding of Reed-Solomon codes," *available online at [www.arxiv.org](http://www.arxiv.org)*, Sept. 2005.
- [33] T. Halford and K. Chugg, "Random redundant soft-in soft-out decoding of linear block codes," in *Proceedings of Int. Symp. on Inform. Theory (ISIT)*, (Seattle, WA), pp. 2230–2234, July 2006.
- [34] M. Schwartz and A. Vardy, "On the stopping distance and stopping redundancy of codes," in *Proc. IEEE International Symposium on Information Theory*, (Adelaide, Australia), pp. 975–979, September 2005.

- [35] H. Hollman and L. Tolhuizen, “On parity check collections for iterative erasure decoding that correct all correctable erasure patterns of a given size,” *submitted to IEEE Trans. on Inform. Theory*, July 2005.
- [36] T. Hehn, S. Laendner, O. Milenkovic, and J. B. Huber, “The stopping redundancy hierarchy of cyclic codes,” in *Proceedings of the 44th Annual Allerton Conference on Communication, Control and Computing*, 2006.
- [37] J. Yedidia, *Advanced Mean Field Methods: Theory and Practice*. Cambridge, MA: MIT Press, 2001.
- [38] R. Cook, *Experts in Uncertainty: Opinion and Subjective Probability in Science*. Oxford University Press, 1991.
- [39] G. Hardy, J. Littlewood, and G. Polya, *Inequalities*. Cambridge University Press, 1997.
- [40] T. Richardson and R. Urbanke, “The capacity of LDPC codes under message passing decoding,” *IEEE Trans. on Inform. Theory*, vol. 47, pp. 599–618, Feb. 2001.
- [41] S.-Y. Chung, T. Richardson, and R. Urbanke, “Analysis of sum-product decoding of low-density parity-check codes using a gaussian approximation,” *IEEE Trans. on Inform. Theory*, vol. 47, pp. 657–670, Feb. 2001.
- [42] N. Wiberg, *Codes and Decoding on General Graphs*. PhD thesis, Linköping University, Linköping, Sweden, 1996.
- [43] K. Xie and J. Li, “On accuracy of Gaussian assumption in iterative analysis for LDPC codes,” in *Proc. IEEE Intern. Symp. on Inform. Theory (ISIT)*, (Seattle, Washington), July 9-14 2006.
- [44] S. Sankaranarayanan, S. K. Chilappagari, R. Radhakrishnan, and B. Vasić, “Failures of the Gallager B decoder: Analysis and applications,” in *UCSD Center for Information Theory and its Applications Inaugural Workshop*, (San Diego, CA), February 6-9 2006.
- [45] A. Hedayat, N. Sloane, and J. Stufken, *Orthogonal Arrays: Theory and Applications*. New York: Springer Verlag, 1999.
- [46] N. Alon and J. Spencer, *The Probabilistic Method*. Interscience Series in Discrete Mathematics and Optimization, John Wiley, 2000.
- [47] M. Hofri, *Analysis of Algorithms*. Oxford University Press, 1995.
- [48] F. MacWilliams and N. Sloane, *The Theory of Error-Correcting Codes*. North-Holland Publishing Company, 1977.
- [49] Y. Kou, S. Lin, and M. Fossorier, “Low-density parity-check codes based on finite geometries: a rediscovery and new results,” *IEEE Trans. Inform. Theory*, vol. 47, pp. 2711–2736, Nov 2001.
- [50] J. Hirschfeld, *Finite Projective Spaces of Three Dimensions*. Oxford Mathematical Monographs, 1985.
- [51] J. Hirschfeld, *Projective Geometries over Finite Fields*. Oxford Mathematical Monographs, 1998.
- [52] J. Hu, H. Loeliger, J. Dauwels, and F. Kschischang, “A general computation rule for lossy summaries/messages with examples from equalization,” in *Proc. 44th Allerton Conf. on Communication, Control, and Computing*, (Monticello, Illinois, USA), September 2006.